



Deposited via The University of Leeds.

White Rose Research Online URL for this paper:

<https://eprints.whiterose.ac.uk/id/eprint/80222/>

Version: Accepted Version

Article:

Wright, TJ, Elliott, JR, Wang, H et al. (2013) Earthquake cycle deformation and the Moho: Implications for the rheology of continental lithosphere. *Tectonophysics*, 609. 504 - 523.
ISSN: 0040-1951

<https://doi.org/10.1016/j.tecto.2013.07.029>

Reuse

Items deposited in White Rose Research Online are protected by copyright, with all rights reserved unless indicated otherwise. They may be downloaded and/or printed for private study, or other acts as permitted by national copyright laws. The publisher or other rights holders may allow further reproduction and re-use of the full text version. This is indicated by the licence information on the White Rose Research Online record for the item.

Takedown

If you consider content in White Rose Research Online to be in breach of UK law, please notify us by emailing eprints@whiterose.ac.uk including the URL of the record and the reason for the withdrawal request.

Earthquake cycle deformation and the Moho: Implications for the rheology of continental lithosphere.

Tim J. Wright^a, John Elliott^b, Hua Wang^c, Isabelle Ryder^d

^a*COMET+, School of Earth and Environment, University of Leeds, Leeds, UK, LS2 9JT*

^b*COMET+, Department of Earth Sciences, University of Oxford, Oxford, UK, OX1 3PR*

^c*Department of Surveying Engineering, Guangdong University of Technology,
Guangzhou, China*

^d*School of Environmental Sciences, 4 Brownlow St, University of Liverpool, UK, L69
3GP*

Abstract

The last 20 years has seen a dramatic improvement in the quantity and quality of geodetic measurements of the earthquake loading cycle. In this paper we compile and review these observations and test whether crustal thickness exerts any control. We found 78 earthquake source mechanisms for continental earthquakes derived from satellite geodesy, 187 estimates of interseismic “locking depth”, and 23 earthquakes (or sequences) for which post-seismic deformation has been observed. Globally we estimate seismogenic thickness to be 14 ± 5 and 14 ± 7 km from coseismic and interseismic observations respectively. We find that there is no global relationship between Moho depth and the seismogenic layer thickness determined geodetically. We also found no clear global relationship between seismogenic thickness and proxies for the temperature structure of the crust. This suggests that the effect of temperature, so clear in oceanic lithosphere, is masked in the continents by considerable variation in lithology, strain-rate, and/or grain size. Elastic thicknesses from Bouguer gravity are systematically larger than the geode-

tic seismogenic thicknesses but there is no correlation between them. By contrast, elastic thickness from free-air methods are typically smaller than the geodetic estimates of seismogenic layer thickness. Postseismic observations show considerable regional variations, but most long-term studies of large earthquakes infer viscoelastic relaxation in the lower crust and/or upper mantle with relaxation times of a few months to a few hundred years. These are in apparent contradiction with the higher estimates of elastic thickness. Our analysis of the geodetic data therefore supports the “crème brûlée” model, in which the strength of the continental lithosphere is predominantly in the upper seismogenic layer. However, the distribution of geodetic observations is biased towards weaker areas, and faults can also modify the local rheology. Postseismic results could therefore be sampling weak regions within an otherwise strong crust or mantle.

Keywords: Moho, Crustal deformation, Geodesy, Continental Rheology, Elastic Thickness

1. Introduction

The earthquake deformation cycle is typically divided into three phases: The deformation that occurs during an earthquake is referred to as *coseismic*; it is followed by a period of transient *postseismic* deformation, which eventually decays to a steady-state background *interseismic* deformation (e.g. Thatcher and Rundle, 1979). Recent advances in satellite geodesy, and in particular the rapid uptake of interferometric synthetic aperture radar (InSAR), have led to a dramatic increase in the quantity and quality of deformation measurements of the earthquake cycle (e.g. Wright, 2002; Bürgmann

10 and Dresen, 2008; Weston et al., 2012).

11 Owing to the long inter-event time in many fault zones, typically hun-
12 dreds to thousands of years, we do not have deformation observations with
13 modern instruments spanning a complete earthquake cycle for any single
14 fault. Nevertheless, by looking globally we can observe deformation around
15 faults at different stages of the cycle. InSAR is particularly suitable for
16 measuring the large and rapid coseismic displacements associated with con-
17 tinental earthquakes, but has also been valuable in constraining postseismic
18 and interseismic deformation in several cases, particularly for remote faults
19 with minimal ground-based observations. At the same time, thousands of
20 Global Positioning System (GPS) measurements have been made in active
21 fault zones (e.g. Kreemer et al., 2003). These have been particularly valuable
22 for examining the slower, longer-wavelength deformation associated with the
23 interseismic and postseismic phases of the earthquake cycle.

24 In the past decade, the strength of continental lithosphere has been the
25 cause for considerable controversy (e.g. Jackson, 2002; Burov et al., 2006;
26 Jackson et al., 2008; Burov, 2010; Bürgmann and Dresen, 2008). The debate
27 has focused on whether strength resides in a single layer in the upper crust
28 (the “crème brûlée” model) or whether the upper mantle is also strong (the
29 “jelly sandwich” model). Most earthquakes occur in the upper crust; coseis-
30 mic deformation can be used to infer the depth range of faulting and hence
31 the thickness of the seismogenic layer. During the interseismic and postseis-
32 mic periods, deformation occurs in the lower crust and mantle. We can infer
33 the seismogenic thickness from simple elastic models of the interseismic pe-
34 riod; the rates, location and mechanisms of postseismic deformation can be

35 used to place bounds on the strength of the lower crust and upper mantle.

36 In this paper, we compile observations of earthquake cycle deformation
37 from the published literature made in tectonic areas across the planet, and
38 extract key parameters. In particular we examine the thickness of the upper
39 crustal layer that slips in earthquakes but is locked in the interseismic pe-
40 riod, and examine the depth ranges and timescales over which postseismic
41 relaxation has been inferred to occur. We test whether these parameters are
42 related to estimates of Moho depth, elastic thickness, and geothermal gra-
43 dient, estimated independently. Finally, we discuss the implications for the
44 strength of continental lithosphere.

45 **2. Seismogenic thickness constraints from coseismic deformation**

46 During coseismic deformation, the passage of seismic waves through the
47 entire crust and mantle is testament to their elastic behaviour on short time-
48 scales. On longer timescales, elastic stresses are relaxed through temperature-
49 dependent ductile processes such as viscous relaxation (e.g. Rundle and Jack-
50 son, 1977; Pollitz, 1992) and aseismic afterslip (e.g. Scholz and Bilham, 1991;
51 Perfettini and Avouac, 2004). These processes restrict the vast majority of
52 continental earthquakes to the brittle upper crust. The thickness of this seis-
53 mogenic layer (T_s) has previously been estimated by examining earthquake
54 centroid depths (e.g. Maggi et al., 2000; Jackson et al., 2008) determined by
55 inversions of seismic waves that assume a point source for the earthquake.
56 Geodetic methods allow for additional information about the depth distribu-
57 tion of slip in earthquakes. For small events, most studies assume uniform
58 slip on a rectangular dislocation (Okada, 1985). For larger events, detailed

59 slip distributions are often resolved. In most of these cases, information
60 about the maximum depth extent of slip in the earthquake can be retrieved.
61 Although there are fewer geodetic earthquake solutions than seismic sources,
62 the depth range over which seismic slip occurs is arguably more robust.

63 We have updated the list of 58 continental earthquakes ($M_w \gtrsim 5.5$) stud-
64 ied with InSAR from Weston et al. (2011, 2012), with 20 further earthquakes,
65 to give a database of 78 events (Figure 1a). The list is spread slightly un-
66 evenly across strike-slip (Table 1), normal (Table 2) and reverse (Table 3)
67 faulting mechanisms, with 32, 21 and 25 events respectively. For each earth-
68 quake we extract the bottom depth of faulting in the published geodetic
69 model.

70 The majority of studies involve models in which slip is permitted to occur
71 over a distributed region of sub-fault patches. A limitation of surface geode-
72 tic data is that the resolution of slip decreases with depth (e.g. Funning et al.,
73 2005b; Atzori and Antonioli, 2011) and that, consequently, small deep earth-
74 quakes are difficult to record. However, of the 78 continental earthquakes so
75 far measured, the depth extent of faulting is clustered in the depth range 5–
76 25 km, and slip much deeper than this has been shown to be recoverable for
77 subduction events (e.g. Pritchard et al., 2002). The spread of InSAR bottom
78 depths of faulting is normally distributed with a mean of 14 km and a stan-
79 dard deviation of 5 km (Figure 2 inset). The depth distribution of smaller
80 events, which are unlikely to have ruptured the entire width of the seismo-
81 genic crust, is biased towards the shallower range of depths in our database as
82 they are difficult to detect geodetically if they occur in the mid-lower crust.

83 We compare the depth estimates of faulting from InSAR with seismic

84 source models (Tables 1–3; Figure 2), where available (86% of events exam-
85 ined here). To ensure the seismic solutions are robust and reliable, we only
86 use centroid depths from point-source body-wave modelling (typically for
87 smaller events) and distributed slip source models from body-wave/strong
88 motion (for the larger events). For the larger events, we take the bottom
89 depth of faulting in the slip model presented by the authors in each paper,
90 as was done for the InSAR solutions. For the earthquakes with distributed
91 seismic solutions, (circles in Figure 2), there is a one-to-one correlation be-
92 tween the two estimates of bottom depth, with a small bias of 2–3 km towards
93 deeper seismological slip when compared to the bottom depth from InSAR.
94 This slight discrepancy may arise from the poorer depth resolution in the seis-
95 mological solutions, or be because the InSAR models (which typically use
96 homogeneous elastic half-spaces) bias the slip slightly shallower compared
97 to the layered velocity models typically used in the seismology inversions.
98 When the InSAR depths are compared to the seismological centroid depths
99 (squares in Figure 2), the relationship follows a two-to-one ratio, as would
100 be expected if the slip was symmetrically distributed about the centroid in
101 depth and approached the surface.

102 We compare the geodetically-determined bottom depth of rupture given
103 in Tables 1–3 to the crustal thickness from Crust 2.0 (Bassin et al., 2000),
104 for each type of fault mechanism (Figure 3). The maximum depth of slip
105 for the earthquakes with geodetic solutions are mostly in the range 5–25 km,
106 and occur in regions with crustal thickness in the range of 10–75 km. There
107 is a large spread in the data, but we find no systematic relationship between
108 a deeper Moho and the depth extent of faulting.

109 **3. Seismogenic thickness constraints from interseismic deformation**

110 Simple geodynamic models of the entire earthquake cycle, with an elastic
111 lid overlying a viscoelastic (Maxwell) substrate, suggest that the observed
112 deformation is a function of time since the last earthquake (e.g. Savage and
113 Prescott, 1978; Savage, 1990). Observations of focused strain late in the
114 earthquake cycle around many major fault structures and rapid postseismic
115 transients are cannot be explained by these simple models – the former re-
116 quires a high viscosity in the substrate and the latter a low viscosity (e.g.
117 Hetland and Hager, 2006; Takeuchi and Fialko, 2012).

118 The observational data have led to the development of a new generation
119 of earthquake cycle models that are able to predict focused interseismic defor-
120 mation alongside rapid postseismic deformation (Hetland and Hager, 2006;
121 Johnson et al., 2007a; Vaghri and Hearn, 2012; Takeuchi and Fialko, 2012;
122 Yamasaki et al., 2013). These studies suggest that, although the velocities
123 do change throughout the cycle, they are reasonably steady after the initial
124 postseismic transient deformation has decayed. The models partially explain
125 the ubiquity of the classic elastic dislocation model (Savage and Burford,
126 1973), in which interseismic deformation around strike-slip faults is mod-
127 elled as steady creep on a narrow, infinitely-long and deep vertical fault in
128 an elastic half space beneath a locked lid (the other significant factor is its
129 simplicity).

130 We take a pragmatic approach to interseismic deformation, and have
131 searched for all examples that have been modelled either using the simple
132 deep dislocation formulation or an equivalent elastic block model approach.
133 This allows us to examine spatial variations in the ‘locking depth’ parameter

134 in a consistent manner, even if the model is undoubtedly an oversimplifica-
135 tion.

136 We found 187 estimates of interseismic locking depth in ~ 100 publica-
137 tions (Table 4; Figure 1). Of these, 131 were determined as free parameters
138 in inversions of the geodetic data. Regional variations do exist, with locking
139 depths in Iceland being 7 ± 4 km, compared with 20 ± 6 km in the Himalayas,
140 for example. However, in general the values are remarkably consistent, nor-
141 mally distributed with a global mean of 14 ± 7 km (Figure 4). This is remark-
142 ably similar to the global distribution found for the coseismic bottom depths
143 (Figure 2), with the same mean at 14 km. As was the case for earthquake
144 depths, we find no systematic global relationship between locking depth and
145 crustal thickness (Figures 4).

146 **4. Regional variations in seismogenic thickness**

147 To search for any systematic variations in seismogenic thickness, we exam-
148 ine the distribution of coseismic slip and interseismic locking depths in four
149 continental areas for which we have a sufficient number of geodetic results:
150 Iran, the Mediterranean, Tibet and the Western US (Figure 5).

151 For Iran, the 11 earthquakes so far studied are constrained to be shallower
152 than 20 km and match the interseismic locking depths except for two deep
153 outliers (Figure 5). The results indicate a large aseismic lower crust above
154 the Moho, which is at a depth of 40–45 km.

155 The Mediterranean region, which we define broadly to include 16 earth-
156 quakes in Turkey, Greece, Italy and Algeria, has depths of faulting and lock-
157 ing down to 20–25 km, and a relatively narrow aseismic lower crust above a

158 Moho at 30–40 km (Figure 5).

159 The 16 earthquakes with geodetic solutions in Tibet are largely in the
160 upper 25 km of crust, with one event deeper at 31 km (Sichuan), and the
161 interseismic locking depths, reviewed in depth in Searle et al. (2011), cover
162 the same range (Figure 5). However, the Moho for this region is much deeper
163 at 50–70 km, leaving a much thicker aseismic lower crust.

164 Finally, the Western US has a narrower seismogenic layer of 16 km based
165 upon the 9 earthquakes studied in this small region, and similar interseismic
166 locking depths, estimated from extensive geodetic analyses (Figure 5). The
167 crust is 30–35 km thick, suggesting the aseismic lower crust is \sim 15–20 km
168 thick.

169 Our seismogenic layer thicknesses for these regions are similar to those
170 of Maggi et al. (2000), who used seismological constrained centroid depths.
171 Maggi et al. (2000) also had sufficient earthquakes in Africa, the Tien Shan
172 and North India to establish that seismogenic layer thicknesses are larger in
173 these regions. We could not find enough geodetic studies in these regions to
174 independently verify this result.

175 The consistency between interseismic locking depths and the depth ranges
176 of coseismic slip release (Figure 5), which both peak at around 10–20 km for
177 the regions where we have sufficient data, implies that it is reasonable to es-
178 timate earthquake potential using interseismic geodetic measurements. The
179 geodetic data therefore confirm that, for the regions where most continental
180 earthquakes occur, the upper half of the crust is largely seismic and able to
181 accumulate stress elastically over the earthquake cycle. Deformation occurs
182 aseismically and continuously in the lower crust.

183 5. Rheological constraints from postseismic deformation

184 A period of accelerated deformation is observed after many large earth-
185 quakes, in which instantaneous deformation rates are higher than those ob-
186 served before the earthquake. Several mechanisms are likely occurring during
187 this postseismic phase of the earthquake deformation cycle. Over short time
188 scales (up to a few months), the re-equilibration of ground water levels causes
189 a poroelastic effect (e.g. Jónsson et al., 2003; Fialko, 2004). On longer time
190 scales, aseismic creep on the fault plane (afterslip) and viscoelastic relaxation
191 (VER) of the lower crust and mantle are the most significant processes.

192 The postseismic phase of the earthquake cycle is probably the least well
193 observed; we found only 49 studies in the literature in which postseismic
194 observations have been made for at least two months after the event for con-
195 tinental earthquakes. These studies analysed GPS and/or InSAR data from
196 only 19 individual earthquakes and four groups of earthquakes. Furthermore,
197 the lack of consensus on the appropriate methods for modelling postseismic
198 deformation makes it hard to make a systematic comparison between the
199 studies.

200 Most studies of postseismic deformation after large ($M_w \gtrsim 7$) earthquakes
201 infer afterslip or viscoelastic relaxation as a deep process occurring beneath
202 an upper layer that is modelled as a purely elastic layer. In some cases the
203 thickness of this elastic lid is held fixed at the depth of earthquake rupture. In
204 other studies, the elastic lid thickness is allowed to vary as a free parameter.
205 Studies that invoke afterslip split into two camps: some carry out simple
206 kinematic inversions to find the distribution of slip on an extended fault
207 plane that matches the postseismic geodetic observations (e.g. Bürgmann

208 et al., 2002); more rarely, others calculate a prediction for the amount of
209 afterslip expected based on an assumed friction law for the fault plane (e.g.
210 Hearn et al., 2002; Johnson et al., 2009).

211 Even investigations that agree that viscoelastic deformation is the dom-
212 inant process occurring at depth have no consensus as to the appropriate
213 rheology to ascribe to the viscoelastic material. Simple linear Maxwell rhe-
214 ologies are often used in the first instance, but these are typically unable
215 to explain both ‘early’ and ‘late’ postseismic deformation (definitions left
216 deliberately vague): fitting the early part of the postseismic relaxation pe-
217 riod usually requires a lower viscosity than fitting the later part (e.g. Pollitz,
218 2003; Freed and Bürgmann, 2004; Ryder et al., 2007). Freed and Bürgmann
219 (2004) showed that a non-linear power-law rheology (in which strain rate
220 is proportional to $(\text{stress})^n$) could fit both early and late postseismic de-
221 formation observed by GPS after the 1992 Landers and 1999 Hector Mine
222 earthquakes, with $n = 3.5$. For such models to be correct, the stress change
223 during the earthquake must dominate over the background levels of stress
224 in the crust. Alternatively, Pollitz (2003) and others have often applied a
225 Burgers body rheology to explain postseismic deformation. This linear rhe-
226 ology has two effective viscosities, which allow it to relax rapidly in the early
227 period of postseismic relaxation and more slowly later on. Riva and Gov-
228 ers (2009) and Yamasaki and Houseman (2012) point out that the expected
229 temperature structure in the lower crust and mantle can result in multiple
230 effective viscosities for the relaxing layers - colder shallower layers relax more
231 slowly than deeper, hot layers. Therefore, power-law or Burgers rheologies
232 may not be required by the observations, as has previously been argued.

233 Yet a further complication arises because most of these models assume lat-
234 erally homogeneous (layered) structures. Geological evidence suggests that
235 shear zones develop under major crustal faults due to processes including
236 shear heating (e.g. Thatcher and England, 1998) and grain size reduction
237 (Bürgmann and Dresen, 2008, and references therein). Shear zones may
238 cause lateral variations in viscosity that can also explain the geodetic obser-
239 vations of multiple relaxation times (Vaghri and Hearn, 2012; Takeuchi and
240 Fialko, 2012; Yamasaki et al., 2013).

241 The magnitude of the earthquake being studied and the duration of ob-
242 servation are important factors to consider when interpreting models of post-
243 seismic deformation. Other things being equal, small earthquakes will excite
244 less viscous flow than larger earthquakes. One might therefore expect to have
245 to make observations over a longer time period in order to see evidence at the
246 surface for viscoelastic relaxation at depth. By a similar line of reasoning,
247 viscous flow will be excited in deep viscoelastic layers to a lesser extent than
248 in shallow viscoelastic layers, and very large earthquakes may be required
249 to excite motions in deep layers. Again, one would expect to have to ob-
250 serve for longer to detect a viscous flow signal. In summary, when it comes
251 to inferring evidence for viscoelastic relaxation, the observational odds are
252 stacked against small-magnitude earthquakes embedded in the top of a thick
253 elastic upper layer. The optimum case for observing viscoelastic relaxation
254 is a large earthquake occurring in a thin elastic layer.

255 Despite the various difficulties discussed above, we argue that there is
256 some value in attempting to compile and compare observations of postseis-
257 mic deformation globally. In Figure 6, we summarise the results of studies

258 that collectively model postseismic geodetic data for 19 continental earth-
259 quakes (including two earthquake sequences), plus a handful of groups of
260 earthquakes, some of which occurred many decades ago. We are primar-
261 ily interested in the depth ranges, or lithospheric layers (lower crust, upper
262 mantle), in which different postseismic relaxation processes occur, since this
263 gives valuable insight into the strength profile of the crust and upper mantle
264 over the month to decadal time scale. The range of earthquake magnitudes
265 is 5.6 to 7.9, and all case studies use data covering at least two months fol-
266 lowing the earthquake. The majority of these investigations have modelled
267 viscoelastic relaxation (VER) and/or afterslip. The studies that only model
268 a single process, rather than testing for both processes, are indicated in the
269 figure by asterisks. A few studies also model poroelastic rebound.

270 The compilation of postseismic case studies highlights a number of key
271 points. Firstly, even accounting for the large range of earthquake magnitudes
272 and observation periods, there is considerable variation in inferred rheological
273 structure between different regions around the globe (Figure 6). Afterslip is
274 inferred to occur anywhere from the very top of the crust right down to the
275 upper mantle in a few cases, though some authors acknowledge that this very
276 deep apparent afterslip may in fact be a proxy for VER. VER is inferred to
277 occur in the lower crust in some cases (e.g. Ryder et al., 2007; Riva et al.,
278 2007; Ryder et al., 2011; Bruhat et al., 2011), the upper mantle in others (e.g.
279 Freed and Bürgmann, 2004; Biggs et al., 2009; Johnson et al., 2009; Pollitz
280 et al., 2012), and sometimes in both (e.g. Vergnolle et al., 2003; Hearn et al.,
281 2009; Wang et al., 2009b). We note, however, that even if the spatial pattern
282 of the data clearly indicates viscoelastic relaxation, actual viscosity values

283 for a particular layer are commonly poorly-resolved by the data, which leads
284 to some uncertainty in how VER varies with depth. This issue of resolution
285 for postseismic data has been explored in detail by Pollitz and Thatcher
286 (2010). In Figure 6, the dashed yellow lines indicate depth ranges where
287 (a) viscosities are poorly-constrained, and/or (b) viscosities are several times
288 higher than in the other layer. Both cases go under the label of “possible
289 VER”, as opposed to “dominant VER” (solid yellow lines).

290 Since different studies use different data sets with different resolving ca-
291 pabilities, it is important to consider the interpretations for a particular
292 earthquake or region in aggregate. In some regions there is a clear signa-
293 ture of viscoelastic relaxation in the upper mantle. In the Basin and Range
294 province, mantle VER has been clearly inferred in five separate studies of
295 individual earthquakes (Landers 1992, Hector Mine 1997 and Hebgen Lake
296 1959), as well as for groups of historic earthquakes that occurred in the Cen-
297 tral Nevada Seismic Belt. The four Basin and Range studies that infer only
298 afterslip/poroelastic mechanisms (no VER) did not attempt to model VER
299 (Massonnet et al., 1996; Savage and Svarc, 1997; Peltzer et al., 1998; Perfet-
300 tini and Avouac, 2007). A fifth study (Fialko, 2004) does not model VER
301 explicitly, but as a comment on far-field residuals resulting from afterslip-
302 only modelling, mentions that mantle VER may also have occurred. Only
303 one paper concludes VER in the lower crust (Deng et al., 1998), but Pollitz
304 et al. (2000) and Pollitz (2003) suggest that VER may have occurred in the
305 lower crust as well as the upper mantle, with viscosities at least a factor of
306 two higher in the lower crust. The other earthquake that seems to offer clear
307 evidence for upper mantle VER is the 2002 Denali earthquake in Alaska.

308 The four studies of this event all infer VER in the mantle, with no flow
309 in the lower crust (e.g. Pollitz, 2005; Freed et al., 2006; Biggs et al., 2009;
310 Johnson et al., 2009). Of those, the three studies that also model afterslip
311 conclude that afterslip in the lower crust accompanied mantle VER. For the
312 1999 Izmit earthquake on the North Anatolian Fault, short time-scale (a few
313 months) observations lead to conclusions of afterslip only (Reilinger et al.,
314 2000; Bürgmann et al., 2002; Hearn et al., 2002), but longer time-scale (a few
315 years) observations lead to inferences of VER in the lower crust and upper
316 mantle (Hearn et al., 2009; Wang et al., 2009b). For two M_w 6.5 earthquakes
317 in Iceland in 2002, Jónsson (2008) infer from four years of geodetic data that
318 VER took place in the upper mantle, although initial data only revealed
319 poroelastic rebound (Jónsson et al., 2003).

320 In some regions there is strong evidence for viscoelastic relaxation having
321 occurred primarily in the lower crust, rather than the upper mantle. Along
322 the San Andreas Fault system, multi-year observations following the 2004
323 Parkfield, 1994 Northridge and 1989 Loma Prieta earthquakes indicate lower
324 crustal VER. Again, there are also studies which only solve for afterslip.
325 The study by Freed (2007), on the other hand, investigated both processes,
326 but concluded that only afterslip occurred during the first two years after
327 the Parkfield earthquake. A later study of the same event by Bruhat et al.
328 (2011) used six years of postseismic data and suggested that VER in the
329 lower crust accompanied afterslip in the upper crust, although the authors
330 acknowledge that observations of localised tremor in the lower crust (Shelly
331 and Johnson, 2011) support the occurrence of deep afterslip. Lower crustal
332 VER has also been inferred in studies of earthquakes in Italy, Taiwan and

333 Tibet. In general, smaller earthquakes do not appear to excite flow in the
334 upper mantle, but larger earthquakes at the same locations may be able to.
335 One earthquake in Tibet where VER has not been inferred at any depth was
336 the 2008 Nima-Gaize event (Ryder et al., 2010). This was a small (M_w 6.4)
337 earthquake and the InSAR data used only covered the first nine postseismic
338 months. Viscoelastic relaxation was not ruled out by these short time-scale
339 data; rather, the lack of VER signature was used to place a lower bound on
340 possible viscosities in the lower crust.

341 Because of the wide variety of approaches used in modelling viscoelastic
342 relaxation, we do not include viscosity values in our compilation in Figure 6.
343 A detailed comparison of modelling efforts is beyond the scope of this pa-
344 per. Nevertheless, it is helpful to consider the range of viscosities inferred in
345 postseismic studies, and identify some general patterns. For the viscoelastic
346 layers (lower crust or upper mantle) where viscosity is well-constrained, the
347 range of Maxwell viscosities across all studies is $1 \times 10^{17} - 7 \times 10^{19}$ Pa s.
348 Where other linear viscoelastic rheologies are used (standard linear solid,
349 Burgers), the range is $1 \times 10^{17} - 2 \times 10^{20}$ Pa s. It should be noted that for
350 poorly-constrained layers, several studies estimate a lower bound. For exam-
351 ple, Gourmelen and Amelung (2005) can only constrain the viscosity of the
352 lower crust in the CNSB to be $> 1 \times 10^{20}$ Pa s. The overall viscosity range for
353 the well-constrained layers gives a range of relaxation times from one month
354 up to 200 years. For the poorly-constrained layers, relaxation times may be
355 longer than 200 years. Many short time scale (< 10 year) studies have con-
356 cluded that apparent viscosity increases with time following an earthquake.
357 However, the modern studies of ongoing relaxation around earthquakes that

358 occurred several decades ago do not consistently find higher viscosities than
359 shorter postseismic studies of more recent earthquakes.

360 To summarise the results from the entire postseismic compilation: of the
361 ~ 20 individual earthquakes/sequences considered, 16 have VER inferred by
362 at least one study. Of the four that do not, two (L'Aquila and Nima-Gaize)
363 are small magnitude (M_w 6.3 and 6.4 respectively) and only have a short
364 period of observation (6 and 9 months respectively), and so would not be
365 expected to have excited observable deep viscous flow. The other two are the
366 Zemmouri and Mozambique earthquakes in Africa. These are larger magni-
367 tude (M_w 6.9 and 7) events and have been observed for longer (at least 2.5
368 years). A broad-brush conclusion is that viscoelastic relaxation in the lower
369 crust and/or upper mantle is to be expected after most large earthquakes
370 (but may only be detected with very long periods of observations). This in
371 turn implies that there is not much long-term strength beneath the elastic
372 upper crust, at least in fault zones.

373 **6. Discussion**

374 *6.1. Influence of the Moho depth and geothermal gradient on the earthquake* 375 *cycle*

376 Our initial aim in this paper, in line with the theme of this special vol-
377 ume, was to test whether crustal thickness had any appreciable influence on
378 the deformation observed during the earthquake cycle. The most robust pa-
379 rameter that we have been able to extract is the thickness of the seismogenic
380 layer, which we find to be consistent between coseismic and interseismic in-
381 vestigations. We find, in line with previous seismic studies (e.g. Maggi et al.,

382 2000; Jackson et al., 2008), that there is no simple global relationship be-
383 tween seismogenic layer thickness and crustal thickness. In fact, seismogenic
384 layer thickness is remarkably constant in the regions where we have sufficient
385 data for robust analysis, whereas crustal thicknesses in the same regions vary
386 by a factor of two or more.

387 Ultimately, the seismogenic layer thickness is limited by the depth at
388 which creep processes allow tectonic stresses to be relieved aseismically and
389 this, in turn, is a function of lithology, grain-size, water content, strain rate
390 and temperature. In the oceanic lithosphere, where lithology is fairly con-
391 stant, temperature is the dominant factor, with earthquakes only occurring
392 in the mantle at temperatures below $\sim 600^\circ\text{C}$ (e.g. McKenzie et al., 2005).
393 We test whether temperature exerts a dominant control globally on seismo-
394 genic layer thickness in continental lithosphere by using direct and indirect
395 measures of crustal heat flow.

396 Firstly, we use a global compilation of direct heat flow measurements by
397 Hasterok and Chapman (2008), updated from Pollack et al. (1993). The heat
398 flow data set is noisy and highly uneven in its distribution, with high sample
399 densities in regions such as Europe and North America and lower sampling
400 in Asia. To provide a continuous grid against which to compare average heat
401 flows with the earthquake depths, we first take median samples of the data at
402 0.5 degree spacing. We then interpolate (Smith and Wessel, 1990) to 1 degree
403 spacing to cover regions in which no direct heat flow data are available. We
404 do not recover an inverse relationship between the deepest extent of faulting
405 and average heat flow (Figure 7).

406 Secondly, we use lithospheric thickness, derived from surface wave tomog-

407 raphy (Priestley and McKenzie, 2006), as a proxy for geothermal gradient;
408 areas with thick lithosphere should have relatively low geothermal gradient
409 and hence have a relatively thick seismogenic layer. We also see no clear re-
410 lationship between lithospheric thicknesses and our estimates of seismogenic
411 thickness (Figure 7).

412 On a local scale, there is a clear relationship between the geothermal gra-
413 dient and the seismogenic layer thickness. This is clearly shown by microseis-
414 micity studies in regions such as California (e.g. Sibson, 1982; Nazareth and
415 Hauksson, 2004), and Iceland (e.g. Ágústsson and Flóvenz, 2005; Björnsson,
416 2008). But there is no obvious global relationship between thermal structure
417 and seismogenic layer thickness evident in our compilations. The effect of
418 temperature, which is clear in oceanic lithosphere and in small regions, is
419 masked in the continents by spatial variations in lithology, strain-rate, and
420 grain size.

421 *6.2. Seismogenic and elastic thicknesses – implications for the rheology of* 422 *continental lithosphere*

423 Starkly different estimates for elastic thickness (T_e) have been at the core
424 of the debate about the rheology of continental lithosphere (e.g. Burov and
425 Watts, 2006; Jackson et al., 2008). Several different methods have been used
426 to derive T_e . One method, probably the most commonly applied, relies on
427 the spectral coherence between the Bouguer gravity anomaly and topogra-
428 phy (Forsyth, 1985). Audet and Bürgmann (2011) recently used this method
429 to produce a global map of elastic thickness, giving values that are typically
430 much larger than the seismogenic thicknesses estimated in this paper and
431 elsewhere (Figure 5). For example, in Iran, Audet and Bürgmann (2011)

432 estimate T_e at 35-65 km, but no earthquake occurs deeper than ~ 20 km.
433 McKenzie and Fairhead (1997) showed that estimates of T_e obtained from
434 Bouguer gravity anomalies are upper bounds, since short-wavelength topog-
435 raphy has been removed or modified by surface processes. Instead, they
436 advocate using either the admittance between topography and free-air grav-
437 ity or direct flexural models of free-air gravity profiles. These typically yield
438 much lower values for T_e , which are always less than the seismogenic thickness
439 (Figure 5; McKenzie and Fairhead, 1997; Maggi et al., 2000; Jackson et al.,
440 2008; Sloan et al., 2011). However, Pérez-Gussinyé et al. (2004) suggest that
441 the McKenzie and Fairhead (1997) estimates of T_e may, in turn, be biased
442 towards lower values due to differences in windowing between theoretical and
443 observed admittances.

444 No global grid exists for T_e from free-air methods, so we compared the
445 Audet and Bürgmann (2011) global grid with our geodetic estimates of seis-
446 mogenic thickness, T_s (Figure 7), and find that these estimates of T_e are
447 almost always significantly greater than T_s . Furthermore, we find no correla-
448 tion between T_s and T_e derived in this way. By contrast, regional estimates of
449 T_e derived from free-air gravity (Figure 5) are consistently less than geodetic
450 estimates of T_s , as is the case for seismic estimates of T_s . For the regions
451 where there are sufficient geodetic data to estimate T_s , we found it to be
452 fairly constant. Likewise, there is little variation in free-air T_e in these areas.
453 Maggi et al. (2000) found that in regions where deeper earthquakes do occur
454 in the lower crust (Africa, the Tien Shan and North India), T_e estimated
455 from free-air methods is higher, although it is always significantly lower than
456 estimates derived from Bouguer coherence.

457 We do not wish to use this manuscript to question the validity of either
458 method for estimating elastic thickness for the crust, as extensive literature
459 on this already exists (e.g. McKenzie and Fairhead, 1997; Pérez-Gussinyé
460 et al., 2004; Crosby, 2007). Having said that, the widespread inferences
461 of aseismic deformation in the lower crust and upper mantle, required to
462 explain geodetic observations of postseismic motions, are hard to reconcile
463 conceptually with these regions supporting significant topographic loads over
464 geologic timescales: postseismic relaxation times are on the order of a few
465 months to a few hundred years. Geodetic observations of the seismic cycle
466 therefore appear to support the lower estimates of T_e , and hence the concept
467 that the strength of continental lithosphere is concentrated in the upper
468 seismogenic layer (the “crème brûlée” model).

469 Of course, sampling continental rheology through observations of the
470 earthquake loading cycle is an inherently biased process. Earthquakes are
471 not uniformly distributed throughout the continental lithosphere, and pref-
472 erentially sample areas with lower T_e estimated with from either Bouguer or
473 Free-air gravity methods (e.g. Figure 1), presumably because earthquakes
474 are occurring in the weakest regions (e.g. Tesauro et al., 2012). In addition,
475 fault zones are capable of modifying their local rheology through processes
476 such as shear heating and grain size reduction, which act to create local
477 weak shear zones at depth (Bürgmann and Dresen, 2008). Observations of
478 postseismic relaxation could therefore be sampling weak regions within an
479 otherwise strong crust or mantle (the “banana split” model of Bürgmann
480 and Dresen (2008)). This is consistent with studies of glacial isostatic ad-
481 justment, which often suggest thick elastic lids (e.g. Watts et al., 2013). If

482 only fault zones are weak, topographic loads could still be supported over
483 geologic timescales by stronger regions away from them and higher estimates
484 of T_e could be valid. Such a view would be consistent with the idea that
485 the continents behave as a series of independent crustal blocks (e.g. Meade,
486 2007a; Thatcher, 2007). Dense geodetic observations of deformation in re-
487 gions including Greece, Tibet and the Basin and Range, however, suggest
488 that such blocks are small, if they exist, with dimensions comparable to the
489 thickness of the crust (e.g. Floyd et al., 2010; Hammond et al., 2011; Wang
490 and Wright, 2012).

491 **7. Conclusions**

492 We have compiled geodetic estimates of seismogenic layer thickness from
493 the coseismic and interseismic phases of the earthquake loading cycle, and
494 find no significant relationship with the depth of the Moho. For the regions
495 where there are sufficient geodetic data to obtain robust results, the seismo-
496 genic layer thickness determined from both coseismic geodetic slip inversions
497 and interseismic locking depth analyses are reasonably constant between re-
498 gions, despite considerable variation in crustal thickness.

499 We find rupture depths inferred from coseismic geodetic slip inversions
500 to be consistent with depths from seismology bodywave inversions. In the
501 regions where there are sufficient data, the interseismic “locking depth” es-
502 timates are also consistent with the seismogenic layer thickness found co-
503 seismically. This implies that interseismic geodetic observations are reliable
504 indicators of earthquake potential.

505 The transition from frictional controlled faulting to aseismic creeping pro-

506 cesses usually occurs in the mid crust and is thought to be dependent on
507 lithology, strain-rate, grain-size, water content and temperature. We found
508 no relationship between the seismogenic thickness and geothermal gradient
509 (measured directly or inferred from lithospheric thickness models). This sug-
510 gests that the effect of temperature, which is so clear in oceanic lithosphere,
511 is masked in the continents by considerable variation in lithology, strain-rate
512 and grain size.

513 Elastic thicknesses derived from the coherence between Bouguer grav-
514 ity and topography are systematically larger than the seismogenic thickness
515 estimated geodetically, but there is no obvious correlation between them.
516 By contrast, as has previously been shown, elastic thicknesses from free-air
517 gravity methods are typically smaller than seismogenic layer thicknesses; al-
518 though there are no geodetic results in regions where Maggi et al. (2000)
519 found high T_e and high T_s , the consistency of seismogenic thicknesses from
520 geodesy and seismology suggests that this relationship will hold.

521 The rapid relaxation of the lower crust and/or upper mantle observed in
522 many places is hard to reconcile with the higher estimates of T_e – relaxation
523 times are typically observed to be a few months to a few centuries. Our
524 analysis of the geodetic data therefore supports the “*crème brûlée*” model,
525 in which the strength of the continental lithosphere is supported in the upper
526 seismogenic layer.

527 However, we note that geodetic observations of the earthquake cycle are
528 inherently biased in their distribution. Furthermore, fault zones modify the
529 rheology of the crust and mantle in which they sit through processes includ-
530 ing grain-size reduction and shear heating. The weak material that responds

531 in the postseismic period may therefore not be representative of the bulk
532 rheology of the continental lithosphere: Postseismic results could be sam-
533 pling weak regions within an otherwise strong crust or mantle (the “banana
534 split” model of Bürgmann and Dresen (2008)). Studies of glacial or lake
535 loading/unloading may not suffer from this bias.

536 Our compilation suffers from the relatively short time that satellite geode-
537 tic methods have been available, a lack of truly global coverage (in compar-
538 ison to seismology), and from the variations in modelling strategies applied
539 by different groups. Specifically, we lack sufficient geodetic observations from
540 areas where Maggi et al. (2000) and others have inferred thicker seismogenic
541 layers. In addition, postseismic deformation results are too scarce, and mod-
542 elling strategies too variable, to form a robust global picture. With the start
543 of the 20-year Sentinel-1 SAR satellite program in 2013, systematic, dense
544 geodetic observations will be made globally for the first time, dramatically
545 increasing the availability and reliability of geodetic observations of the earth-
546 quake loading cycle. We strongly recommend that the geodetic community
547 follows the lead of the seismological community by measuring, modelling and
548 cataloguing coseismic, interseismic and postseismic deformation in a routine,
549 systematic fashion.

550 **8. Acknowledgments**

551 This work was supported in part by the Natural Environmental Research
552 Council (NERC) through the National Centre of Earth Observation (NCEO)
553 of which the Centre for the Observation and Modelling of Earthquakes, Vol-
554 canoes & Tectonics (COMET, <http://comet.nerc.ac.uk>) is a part. Crust 2.0

555 (Bassin et al., 2000) was downloaded from <http://igppweb.ucsd.edu/~gabi/rem.html>.
556 We are grateful to Pascal Audet and Roland Bürgmann for making their
557 global Elastic Thickness dataset available, and to Dan McKenzie and Keith
558 Priestley for sharing their lithospheric thickness data. Global heat flow data
559 were taken from the Global Heat Flow Database of the International Heat
560 Flow Commission (www.heatflow.und.edu). This manuscript was improved
561 by constructive reviews from Roland Bürgmann and an anonymous reviewer,
562 and we are grateful for additional comments from Tony Watts, Alex Cop-
563 ley and Al Sloan. Most figures were made using the public domain Generic
564 Mapping Tools (Wessel and Smith, 1998). TJW was funded by the Royal
565 Society through a University Research Fellowship. HW is supported by the
566 NSFC (41104016).

Table 1: Compilation of continental strike-slip earthquakes studied with InSAR, updated from Weston et al. (2011, 2012) to include the bottom depth of faulting (D) and more recent InSAR constrained source models. The type of model used is denoted by uniform (U) or distributed (D) slip. Seismological source model depths (Z) are given where available as centroid depths for points sources or bottom depths for finite fault planes, the latter denoted by an asterisk.

#	Name	M_w	Date	Lat.	Lon.	D (km)	Slip	Reference	Z (km)	Reference
1	Landers, CA., USA	7.3	1992/06/28	34.45	243.48	15	D	Fialko (2004)	15*	Wald and Heaton (1994)
2	Al Hoceima, Morocco	6.0	1994/05/26	35.20	355.94	12	U	Biggs et al. (2006)	8	Biggs et al. (2006)
3	Double Spring Flat, NV., USA	6.0	1994/09/12	38.82	240.38	12	U	Amelung and Bell (2003)	6	Ichinose et al. (1998)
4	Kobe, Japan	6.9	1995/01/17	34.62	135.06	15	U	Ozawa et al. (1997)	20*	Ide et al. (1996)
5	Neftegorsk, Sakhalin, Russia	7.2	1995/05/27	52.89	142.90	22	U	Tobita et al. (1998)	9	Katsumata et al. (2004)
6	Nuweiba, Egypt	7.3	1995/11/22	28.88	34.75	20	D	Baer et al. (2008)	15	Hofstetter et al. (2003)
7	Kagoshima-kenhokuseibu, Japan	6.1	1997/03/26	31.98	130.40	14	U	Fujiwara et al. (1998)	11*	Horikawa (2001)
8	Zirkuh, Iran	7.2	1997/05/10	33.40	59.96	18	D	Sudhaus and Jónsson (2011)	13	Berberian et al. (1999)
9	Manyi, Tibet	7.5	1997/11/08	35.22	87.15	20	D	Funning et al. (2007)	12	Velasco et al. (2000)
10	Fandoqa, Iran	6.6	1998/03/14	30.01	57.64	7	U	Berberian et al. (2001)	5	Berberian et al. (2001)
11	Aiquile, Bolivia	6.6	1998/05/22	-17.89	294.85	14	D	Funning et al. (2005a)	-	-
12	Izmit, Turkey	7.4	1999/08/17	40.72	30.07	20	D	Çakir et al. (2003)	12*	Li et al. (2002)
13	Hector Mine, CA., USA	7.1	1999/10/16	34.56	243.73	14	D	Simons et al. (2002)	15*	Ji et al. (2002)
14	Düzce, Turkey	7.1	1999/11/12	40.72	31.26	18	D	Burgmann et al. (2002)	22*	Umutlu et al. (2004)
15	South Seismic Zone, Iceland	6.5	2000/06/17	63.97	339.66	10	D	Pedersen et al. (2001)	-	-
16	South Seismic Zone, Iceland	6.4	2000/06/21	63.98	339.30	10	D	Pedersen et al. (2001)	-	-
17	Kokoxili, Tibet	7.8	2001/11/14	35.84	92.45	20	D	Lasserre et al. (2005)	24*	Antolik et al. (2004)
18	Nenana Mountain, AK, USA	6.7	2002/10/23	63.50	211.95	24	D	Wright et al. (2003)	-	-
19	Denali, AK, USA	7.9	2002/11/03	63.22	214.85	20	D	Wright et al. (2004a)	30*	Oglesby et al. (2004)
20	Siberian Altai, Russia	7.2	2003/09/27	49.9	87.9	15	U	Nissen et al. (2007)	18	Nissen et al. (2007)
21	Bam, Iran	6.6	2003/12/26	29.03	58.36	15	D	Funning et al. (2005b)	7	Jackson et al. (2006)
22	Al Hoceima, Morocco	6.4	2004/02/24	35.14	356.00	18	D	Biggs et al. (2006)	8	Biggs et al. (2006)
23	Parkfield, CA., USA	6.0	2004/09/28	35.8	239.6	15	D	Johanson et al. (2006)	12*	Langbein et al. (2005)
24	Chalan, Chulan, Iran	6.1	2006/03/31	33.67	48.88	9	D	Peyret et al. (2008)	6	Peyret et al. (2008)
25	South-West Iceland	6.1	2008/05/29	63.9	338.9	6	D	Decriem et al. (2010)	-	-
26	Port-au-Prince, Haiti	7.1	2010/01/12	18.5	287.4	20	D	Calais et al. (2010)	22*	Hayes et al. (2010)
27	El-Mayor Cucapah, Baja, Mexico	7.1	2010/04/04	32.2	244.7	16	D	Wei et al. (2011)	-	-
28	Yushu, China	6.8	2010/04/13	33.10	96.70	18	D	Li et al. (2011)	6	Li et al. (2011)
29	Darfield, New Zealand	7.1	2010/09/03	-43.58	172.19	14	D	Elliott et al. (2012)	7	Elliott et al. (2012)
30	Rigan, Iran	6.5	2010/12/20	28.25	59.12	13	D	Walker et al. (2013)	5	Walker et al. (2013)
31	Rigan, Iran	6.2	2011/01/27	28.15	59.04	17	D	Walker et al. (2013)	9	Walker et al. (2013)
32	Shan, Burma	6.8	2011/03/24	99.99	20.67	13	D	Feng et al. (2013)	-	-

Table 2: Compilation of continental normal faulting earthquakes studied with InSAR. Rest of caption as for Table 1.

#	Name	M_w	Date	Lat.	Lon.	D (km)	Slip	Reference	Z (km)	Reference
1	Little Skull Mountain, CA, USA	5.6	1992/06/29	36.75	243.76	13	U	Lohman et al. (2002)	8	Romanowicz et al. (1993)
2	Nyemo, Tibet	6.1	1992/07/30	29.7	90.2	12	U	Elliott et al. (2010)	10	Elliott et al. (2010)
3	Ngamring County, Tibet	6.1	1993/03/20	29.06	87.48	9	U	Funning (2005)	-	-
4	Eureka Valley, CA., USA.	6.1	1993/05/17	37.11	242.21	12	U	Massonnet and Feigl (1995)	-	-
5	Grevena, Greece	6.6	1995/05/13	40.1	21.7	15	D	Rigo et al. (2004)	11	Hatzfeld et al. (1997)
6	Aigion, Greece	6.2	1995/06/15	38.33	22.22	10	U	Bernard et al. (1997)	7	Bernard et al. (1997)
7	Dinar, Turkey	6.3	1995/10/01	38.10	30.08	13	U	Wright et al. (1999)	4	Wright et al. (1999)
8	Colfiorito, Italy	5.7	1997/09/26	43.0	12.9	7	D	Stramondo et al. (1999)	7	Hernandez et al. (2004)
9	Colfiorito, Italy	6.0	1997/09/26	43.1	12.9	7	D	Stramondo et al. (1999)	7	Hernandez et al. (2004)
10	Athens, Greece	6.0	1999/09/07	38.1	23.6	12	U	Kontoes et al. (2000)	10	Louvari and Kiratzi (2001)
11	Cankiri, Turkey	6.0	2000/06/06	40.65	33.05	8	U	Cakir and Akoglu (2008)	15*	Utkucu et al. (2003)
12	Zhongba, Tibet	6.2	2004/07/11	30.7	83.75	17	D	Elliott et al. (2010)	9	Elliott et al. (2010)
13	Zhongba, Tibet	6.2	2005/04/07	30.45	83.75	11	D	Elliott et al. (2010)	5	Elliott et al. (2010)
14	Machaze, Mozambique	7.0	2006/02/22	-21.2	33.4	25	D	Copley et al. (2012)	15	Yang and Chen (2008)
15	Gerze, Tibet	6.4	2008/01/09	32.4	85.3	12	D	Elliott et al. (2010)	11	Elliott et al. (2010)
16	Gerze, Tibet	5.9	2008/01/16	32.45	85.25	6	D	Elliott et al. (2010)	6	Elliott et al. (2010)
17	Yutian, Tibet	7.1	2008/03/20	35.4	81.5	14	D	Elliott et al. (2010)	7	Elliott et al. (2010)
18	Zhongba, Tibet	6.7	2008/08/25	30.8	83.5	19	D	Elliott et al. (2010)	8	Elliott et al. (2010)
19	Damxung, Tibet	6.3	2008/10/06	29.8	90.4	14	D	Elliott et al. (2010)	7	Elliott et al. (2010)
20	L'Aquila, Italy	6.3	2009/04/06	42.33	13.45	13	D	Walters et al. (2009)	17	Cirella et al. (2009)
21	Karonga, Malawi	6.0	2009/12/19	-10.0	34.9	6	D	Biggs et al. (2010)	5	Biggs et al. (2010)

Table 3: Compilation of continental reverse faulting earthquakes studied with InSAR. Rest of caption as for Table 1.

#	Name	M_w	Date	Lat.	Lon.	D (km)	Slip	Reference	Z (km)	Reference
1	Fawnskin, CA., USA	5.4	1992/12/04	34.35	243.09	4	U	Feigl et al. (1995)	12	Jones and Hough (1995)
2	Killari, India	6.1	1993/09/29	18.0	76.5	6	U	Satyabala (2006)	3	Seeber et al. (1996)
3	Northridge, CA., USA	6.7	1994/01/17	34.3	241.5	14	U	Massonnet et al. (1996)	22*	Dreger (1994)
4	Sefidabeh, Iran	6.1	1994/02/23	30.9	60.5	13	D	Parsons et al. (2006)	7	Berberian et al. (2000)
5	Sefidabeh, Iran	6.2	1994/02/24	30.85	60.5	10	D	Parsons et al. (2006)	10	Berberian et al. (2000)
6	Sefidabeh, Iran	6.0	1994/02/26	30.8	60.5	13	D	Parsons et al. (2006)	5	Berberian et al. (2000)
7	Zhangbei-Shangyi, China	5.7	1998/01/10	41.14	114.44	8	D	Li et al. (2008)	-	-
8	Mt Iwate, Japan	6.1	1998/09/03	39.80	140.90	5	D	Nishimura et al. (2001)	6*	Nakahara et al. (2002)
9	Chamoli, India	6.4	1999/03/28	30.44	79.39	13	U	Satyabala and Bilham (2006)	-	-
10	Ain Temouchent, Algeria	5.7	1999/12/22	35.2	-1.3	8	D	Belabbès et al. (2009a)	4	Yelles-Chaouche et al. (2004)
11	Bhuj, India	7.6	2001/01/26	23.51	70.27	25	D	Schmidt and Bürgmann (2006)	26*	Antolik and Dreger (2003)
12	Boumerdes-Zemmouri, Algeria	6.9	2003/05/21	36.8	3.7	20	D	Belabbès et al. (2009b)	23*	Semmane et al. (2005)
13	Miyagi, Japan	6.4	2003/07/26	38.45	141.19	6	U	Nishimura et al. (2003)	9*	Hikima and Koketsu (2004)
14	Niigata, Japan	6.8	2004/10/23	37.30	138.83	9	U	Ozawa et al. (2005)	13*	Asano and Iwata (2009)
15	Dahuiyeh (Zarand), Iran	6.4	2005/02/22	31.50	56.80	9	U	Talebian et al. (2006)	7	Talebian et al. (2006)
16	Kashmir, Pakistan	7.6	2005/10/08	34.29	73.77	14	D	Pathier et al. (2006)	17*	Avouac et al. (2006)
17	Qeshm, Iran	6.0	2005/11/27	26.88	55.89	9	U	Nissen et al. (2010)	9	Nissen et al. (2010)
18	Qeshm, Iran	6.0	2006/06/28	26.91	55.89	12	U	Nissen et al. (2010)	11	Nissen et al. (2010)
19	Noto Hanto, Japan	6.9	2007/03/25	37.22	136.66	15	U	Fukushima et al. (2008)	20*	Horikawa (2008)
20	Sichuan, China	7.9	2008/05/12	31.77	104.23	31	D	Hao et al. (2009)	35*	Nakamura et al. (2010)
21	Qeshm, Iran	6.0	2008/09/10	26.88	55.89	8	U	Nissen et al. (2010)	8	Nissen et al. (2010)
22	Qaidam, Tibet	6.3	2008/11/10	37.55	95.85	22	U	Elliott et al. (2011)	18	Elliott et al. (2011)
23	Qaidam, Tibet	6.3	2009/08/28	37.55	95.85	12	U	Elliott et al. (2011)	5	Elliott et al. (2011)
24	Christchurch, New Zealand	6.3	2011/02/21	-43.55	172.7	10	D	Elliott et al. (2012)	9*	Holden (2011)
25	Van, Turkey	7.1	2011/10/23	38.71	43.37	25	D	Elliott et al. (2013)	20	Elliott et al. (2013)

Table 4: Compilation of interseismic parameters studied with geodetic data. Double lines separate regions of Tibet, Himalayas and Baikal-Mongolia.

#	Fault Name	Lon ($^{\circ}$ E)	Lat ($^{\circ}$ N)	Data Source	D (km)	Reference
1	Altyn Tagh	79.5	36	InSAR92-99	10*	Wright et al. (2004b)
2	Altyn Tagh	85	37	InSAR93-00	15*	Elliott et al. (2008)
3	Altyn Tagh	90	38.6	GPS94-98	8-36	Bendick et al. (2000)
4	Altyn Tagh	90	38.6	GPS94-02	20	Wallace et al. (2004)
5	Altyn Tagh	90	38.6	GPS98-04	15*	Zhang et al. (2007)
6	Altyn Tagh	94	39.3	GPS98-04	15*	Zhang et al. (2007)
7	Altyn Tagh	94	39	InSAR95-06	7-9	Jolivet et al. (2008)
8	Altyn Tagh	96	40	GPS98-04	15*	Zhang et al. (2007)
9	Haiyuan	104	37	InSAR93-98	0-4.2	Cavalié et al. (2008)
10	Karakoram	78.8	33.5	InSAR92-99	10*	Wright et al. (2004b)
11	Karakoram	78.0	34.0	InSAR92-10	15*	Wang and Wright (2012)
12	Lamu Co	82.5	32.5	InSAR92-99	3-5.8	Taylor and Peltzer (2006)
13	Gyaring Co	87.5	31.5	InSAR92-99	23-27	Taylor and Peltzer (2006)
14	Riganpei Co	85.75	32.5	InSAR92-99	14.5	Taylor and Peltzer (2006)
15	Kunlun	94	35	GPS98-04	15*	Kirby et al. (2007)
16	Kunlun	101.5	34	GPS98-04	15*	Kirby et al. (2007)
17	Kunlun	102.5	34	GPS98-04	15*	Kirby et al. (2007)
18	Manyi	87	35.2	InSAR92-97	22 \pm 15	Bell et al. (2011)
19	Xianshuihe	101.2	31	GPS -07	9.2 \pm 3.7	Meng et al. (2008)
20	Xianshuihe	101.8	30.3	GPS -07	1.0 \pm 0.6	Meng et al. (2008)
21	Xianshuihe	100.5	31.5	GPS98-04& InSAR96-08	3-6	Wang et al. (2009a)
22	Block	84	30	GPS91-00	15*	Chen et al. (2004)
23	Block	88	35	GPS98-04	17*	Meade (2007b)
24	Block	91	35	GPS&Geology	16*	Loveless and Meade (2011)
25	MHT	81-88	27.5-30	GPS91-94	20 \pm 4	Bilham et al. (1997)
26	W. MHT	79-84	28-30	GPS91-97	25.0	Larson et al. (1999)
27	W. MHT	84-92	27-28	GPS91-97	16.2	Larson et al. (1999)
28	W. MHT	76.0-80.3	29.2-33.0	GPS95-00	15	Banerjee and Bürgmann (2002)
29	W. MHT	80-84	28.2-30.0	GPS95-00	20-21	Jouanne et al. (2004)
30	W. MHT	84-90	26.5-28.2	GPS95-00	17-21	Jouanne et al. (2004)
31	W. MHT	76-83	28.5-31.5	GPS91-00	18.3	Chen et al. (2004)
32	W. MHT	83-89	27.5-28.5	GPS91-00	14.3	Chen et al. (2004)
33	W. MHT	79.5-83.5	28.0-30.0	GPS95-01	12.1	Bettinelli et al. (2006)
34	W. MHT	83.5-87.2	27.0-28.0	GPS95-01	20.4	Bettinelli et al. (2006)
35	W. MHT	79.0-89.6	27.1-28.3	GPS95-07	24.1	Banerjee et al. (2008)
36	W. MHT	78.4-84	28.5-31.5	GPS93-11	15-20	Ader et al. (2012)
37	W. MHT	84-88.1	27.5-28.5	GPS93-11	15-20	Ader et al. (2012)
38	E. MHT	89-94	27.0-27.6	GPS91-00	20.3	Chen et al. (2004)
39	E. MHT	90.0-99.8	26.9-28.5	GPS95-07	20.0	Banerjee et al. (2008)
40	Dauki	90.1-93.0	25.5-25.3	GPS95-07	37.7	Banerjee et al. (2008)
41	Bolnay	98	49.5	GPS94-02	35*	Calais et al. (2003)
42	Gobi Altai	98	45.5	GPS94-02	35*	Calais et al. (2003)
43	Tunka	101	52	GPS94-02	35*	Calais et al. (2003)
44	Baikal rift	107	53	GPS94-02	35*	Calais et al. (2003)

Table 4: Compilation of interseismic parameters studied with geodetic data (continued).

Double lines separate regions of Iran, Mediterranean and New Zealand.

#	Fault Name	Lon ($^{\circ}$ E)	Lat ($^{\circ}$ N)	Data Source	D (km)	Reference
45	MZP	57.2	27	GPS00-02	10-15	Bayer et al. (2006)
46	MZP	57.2	27	GPS00-08	15	Peyret et al. (2009)
47	SKJ	58	27	GPS00-02	15*	Bayer et al. (2006)
48	SKJ	57.7	27.7	GPS00-08	30	Peyret et al. (2009)
49	Khazar	51.5	36.7	GPS00-08	33	Djamour et al. (2010)
50	Khazar	52	36.5	GPS00-08	10	Djamour et al. (2010)
51	NTF	45	39	GPS99-09	15.5	Djamour et al. (2011)
52	NTF	47	37.5	GPS99-09	14	Djamour et al. (2011)
53	MRF	50	32	GPS97-03	10*	Walpersdorf et al. (2006)
54	MRF	54	29.5	GPS97-03	10*	Walpersdorf et al. (2006)
55	Doruneh	57	35	InSAR03-10	12*	Pezzo et al. (2012)
56	N. MMF	27.5	40.8	InSAR92-03	9-17	Motagh et al. (2007)
57	N. MMF	28	40.8	GPS88-97	10.5	Le Pichon et al. (2003)
58	NAF	37	40.5	GPS06-08	12.8 \pm 3.9	Tatar et al. (2012)
59	NAF	38	40.25	GPS06-08	9.4 \pm 3.5	Tatar et al. (2012)
60	NAF	39.2	39.9	GPS06-08	8.1 \pm 3.3	Tatar et al. (2012)
61	NAF	38.8	39.9	InSAR92-99	5-33	Wright et al. (2001)
62	NAF	38.8	39.9	InSAR92-99	13.5-25	Walters et al. (2011)
63	NAF	32.5	40.8	InSAR92-02	14	Çakir et al. (2005)
64	Block	28	40.5	GPS88-97	6.5 \pm 1.1	Meade et al. (2002)
65	Block	29.8	40.6	GPS88-05	18-21*	Reilinger et al. (2006)
66	Yammouneh	36	33-34.5	GPS02-05	13	Gomez et al. (2007)
67	S. DSF	36	29.5-33.5	GPS96-01	12	Wdowinski et al. (2004)
68	S. DSF	36	29.5-33.5	GPS99-05	11.5 \pm 10.2	Le Beon et al. (2008)
69	S. DSF (WAF)	36	29.5-31.5	GPS96-01	15 \pm 5	al Tarazi et al. (2011)
70	S. DSF (JVF)	36	31.5-33.5	GPS96-01	8 \pm 5	al Tarazi et al. (2011)
71	Messina	15.5	38.25	GPS94-09	7.6	Serpelloni et al. (2010)
72	S. Alps	13.2	46.5	GPS96-05	3	D'Agostino et al. (2005)
73	C. Apennines	13.5	42.5	GPS94-10	15*	D'Agostino et al. (2011)
74	Block	35	30	GPS96-03	13*	Mahmoud et al. (2005)
75	Block	36.5	35	GPS88-05	12*	Reilinger et al. (2006)
76	Block	355	35	GPS99-09	15*	Koulali et al. (2011)
77	Block	16	42	GPS	20*	Battaglia et al. (2004)
78	Block	26	39	GPS88-01	10*	Nyst and Thatcher (2004)
79	C. Alpine	170	-43.5	GPS94-98	18	Moore et al. (2002)
80	C. Alpine	170	-43.5	GPS94-98	22 \pm 1	Beavan et al. (1999)
81	C. Alpine	170	-43.5	GPS94-98	6 \pm 1	Beavan et al. (1999)
82	C. Alpine	170	-43.5	GPS01-10	13-18	Beavan et al. (2010)
83	S. Alpine	169	-44	GPS95-98	20 \pm 2	Pearson et al. (2000)
84	S. Alpine	169	-44	GPS95-98	10 \pm 2	Pearson et al. (2000)
85	Awatere	173.5	-42	GPS94-04	13	Wallace et al. (2007)
86	Clarence	173	-42.3	GPS94-04	13	Wallace et al. (2007)
87	Hope	169	-42.6	GPS94-04	20	Wallace et al. (2007)
88	Wairau	173.3	-41.7	GPS94-04	20	Wallace et al. (2007)
89	Apline	170	-43.5	GPS94-04	18	Wallace et al. (2007)

Table 4: Compilation of interseismic parameters studied with geodetic data (continued).

Double lines separate regions of Iceland, Alaska and Western United States.

#	Fault Name	Lon ($^{\circ}$ E)	Lat ($^{\circ}$ N)	Data Source	D (km)	Reference
90	RR	336	63.5	GPS93-04	9.4	Árnadóttir et al. (2009)
91	RPW	337	63.7	GPS92-00	6.6	Árnadóttir et al. (2006)
92	RPW	337	63.7	GPS00-06	4	Keiding et al. (2008)
93	RPW	337	63.7	GPS93-04	7.1	Árnadóttir et al. (2009)
94	RP	338	63.8	GPS92-00	8.3	Árnadóttir et al. (2006)
95	RP	338	63.8	GPS92-00	7	Keiding et al. (2008)
96	RP	338	63.8	GPS93-04	5.3	Árnadóttir et al. (2009)
97	SISZ	339.5	63.8	GPS92-00	19.3	Árnadóttir et al. (2006)
98	SISZ	339.5	63.8	GPS00-06	6	Keiding et al. (2008)
99	SISZ	339.5	63.8	GPS93-04	6.5	Árnadóttir et al. (2009)
100	WVZ	339.5	64.3	GPS94-03	4	LaFemina et al. (2005)
101	WVZ	339.5	64.3	GPS00-06	3	Keiding et al. (2008)
102	WVZ	339.5	64.3	GPS93-04	5.2	Árnadóttir et al. (2009)
103	EVZ	341.5	64	GPS94-03	3	LaFemina et al. (2005)
104	EVZ	341.5	64	GPS93-04	8.9	Árnadóttir et al. (2009)
105	EVZ	341.5	64	GPS94-06	5/3/3	Scheiber-Enslin et al. (2011)
106	NVZ	343.5	65.5	GPS93-04	4.9	Árnadóttir et al. (2009)
107	GL	343	66.5	GPS93-04	13.8	Árnadóttir et al. (2009)
108	HFF	342.5	66.1	GPS93-04	4.7	Árnadóttir et al. (2009)
109	HFF	342.5	66.1	GPS06-10	6.3	Metzger et al. (2011)
110	KR	341.5	66.8	GPS93-04	14.5	Árnadóttir et al. (2009)
<hr/>						
111	Queen Charlotte	227.5	53	GPS98-02	14*	Mazzotti et al. (2003)
112	Queen Charlotte	227.5	53	GPS	10*	Elliott et al. (2010b)
113	Malaspina Fairweather	221	60.2	GPS	5*	Elliott et al. (2010b)
114	Upper Fairweather	221	60.3	GPS	7.6*	Elliott et al. (2010b)
115	C. Fairweather	221	58.5	GPS	10*	Elliott et al. (2010b)
116	Glacier Bay	224	59	GPS	10*	Elliott et al. (2010b)
117	Boundary	223	59.7	GPS	8*	Elliott et al. (2010b)
118	Foothills	222	58.8	GPS	4.98-12*	Elliott et al. (2010b)
119	Fairweather	221	59.7	GPS92-02	9.0 \pm 0.8	Fletcher and Freymueller (2003)
120	Transition	220	58.5	GPS	8/26.5*	Elliott et al. (2010b)
121	Denali	221.5	61	GPS92-02	10*	Fletcher and Freymueller (2003)
122	Denali	221.5	61	GPS	10*	Elliott et al. (2010b)
123	Denali	214	63.5	InSAR92-02	10*	Biggs et al. (2007)
<hr/>						
124	Wasatch	248	40	GPS96-08	7 \pm 3	Soledad Velasco et al. (2010)
125	Imperial	244.5	32.8	GPS99-00	10	Lyons et al. (2002)
126	Imperial	244.5	32.7	GPS	5.9 \pm 3	Smith-Konter et al. (2011)
127	SAF	244.2	33.5	InSAR92-00	17	Fialko (2006)
128	SM	244.2	32.8	GPS	10.8 \pm 1.1	Smith-Konter et al. (2011)
129	ETR	244	34.0	GPS94-09	15*	Spinler et al. (2010)
130	Borrego	244	33.2	GPS	6.4 \pm 1.4	Smith-Konter et al. (2011)
131	DV-FC	244	35.5	GPS94-99	15*	Gan et al. (2000)
132	DV	244	35.5	GPS99-03	12*	Wernicke et al. (2004)
133	DV-FC	244	35.5	GPS	7.5 \pm 2.7	Hill and Blewitt (2006)

Table 4: Compilation of interseismic parameters studied with geodetic data (continued).

Double lines separate regions of Western United States, Sumatran and Southeast Asia.

#	Fault Name	Lon ($^{\circ}$ E)	Lat ($^{\circ}$ N)	Data Source	D (km)	Reference
134	Coachella	244	33.7	GPS	11.5 \pm 0.5	Smith-Konter et al. (2011)
135	SJF	244	33.2	InSAR92-00	12	Fialko (2006)
136	Coyote Creek	243.7	33.2	GPS	6.3 \pm 2	Smith-Konter et al. (2011)
137	Anza	243.5	33.5	GPS	13.7 \pm 3.2	Smith-Konter et al. (2011)
138	YM	243.5	36.8	GPS	12.8 \pm 2.3	Hill and Blewitt (2006)
139	SP	243.5	36.7	GPS99-03	12*	Wernicke et al. (2004)
140	Palm Springs	243.5	34	GPS	16.4 \pm 8	Smith-Konter et al. (2011)
141	SB	243	34	GPS	17.8 \pm 2	Smith-Konter et al. (2011)
142	PV-HM	243	36	GPS94-99	15*	Gan et al. (2000)
143	PV-HM	243	36	GPS	8.6 \pm 3.7	Hill and Blewitt (2006)
144	SJV	243	34.8	GPS	21.5 \pm 6.3	Smith-Konter et al. (2011)
145	SJM	242.5	34	GPS	21.0 \pm 3.2	Smith-Konter et al. (2011)
146	LL-BW	242.5	35.5	InSAR92-00	5	Peltzer et al. (2001)
147	HM	242.2	36.6	InSAR92-00	2 \pm 0.4	Gourmelen et al. (2010)
148	OV	242	36	GPS	7.3 \pm 4.0	Hill and Blewitt (2006)
149	OV	242	36	GPS94-99	15*	Gan et al. (2000)
150	Mojave	242	34.5	GPS	15*	Johnson et al. (2007b)
151	Mojave	242	34.5	GPS	18-24	Johnson et al. (2007b)
152	Mojave	242	34.5	GPS	16.8 \pm 0.4	Smith-Konter et al. (2011)
153	Carrizo	240.5	35	GPS	18.7 \pm 2	Smith-Konter et al. (2011)
154	SA	240	35	GPS	10.2 \pm 3.8	Hill and Blewitt (2006)
155	GVF	237.7	38.4	GPS/InSAR	5	Jolivet et al. (2009)
156	RCF	237.5	38.2	GPS/InSAR	10	Jolivet et al. (2009)
157	SAF	237.2	38	GPS/InSAR	10 \pm 2	Jolivet et al. (2009)
158	Block	242	39	GPS	15*	Hammond et al. (2011)
159	Block	241	40	GPS	15*	Hammond and Thatcher (2007)
160	Sumatran	100	0	GPS89-93	15	Prawirodirdjo et al. (1997)
161	Sumatran	100.7	-0.8	GPS89-96	22 \pm 12	Genrich et al. (2000)
162	Sumatran	100.4	-0.4	GPS89-96	24 \pm 13	Genrich et al. (2000)
163	Sumatran	100	0.6	GPS89-96	56 \pm 35	Genrich et al. (2000)
164	Sumatran	99.4	1.3	GPS89-96	21 \pm 12	Genrich et al. (2000)
165	Sumatran	98.8	2.2	GPS89-96	9 \pm 3	Genrich et al. (2000)
166	Sumatran	98.4	2.7	GPS89-96	9 \pm 4	Genrich et al. (2000)
167	Sagaing	96	22	GPS98-00	15	Vigny et al. (2003); Socquet et al. (2006b)
168	Sagaing	96	26	GPS05-08	7.7	Maurin et al. (2010)
169	Sagaing	96	24	GPS05-08	6.3	Maurin et al. (2010)
170	Sagaing	96	22	GPS05-08	20.3	Maurin et al. (2010)
171	Palu-Koro	120	-1	GPS92-05	12	Socquet et al. (2006a)
172	Gorontalo	122.5	1	GPS92-05	10	Socquet et al. (2006a)
173	Lawanopo	122	-3	GPS92-05	15	Socquet et al. (2006a)
174	Tomini	122	-0.3	GPS92-05	15	Socquet et al. (2006a)

Table 4: Compilation of interseismic parameters studied with geodetic data (continued).

Double lines separate regions of Central America and Taiwan.

#	Fault Name ¹	Lon (°E)	Lat (°N)	Data Source	D (km)	Reference
175	El Pilar	296.5	10.5	GPS94-00	14±2	Pérez et al. (2001)
176	Septentrional	288	20	GPS86-95	15	Dixon et al. (1998)
177	Septentrional	288	20	GPS94-01	15*	Calais et al. (2002)
178	Enriquillo	287	18.5	GPS86-95	15	Dixon et al. (1998)
179	Enriquillo	287	18.5	GPS94-01	15*	Calais et al. (2002)
180	NH	288	20.4	GPS86-95	15	Dixon et al. (1998)
181	NH	288	20.4	GPS94-01	15*	Calais et al. (2002)
182	PMFS	270.5	15	GPS99-03	21	Lyon-Caen et al. (2006)
183	PMFS	270.5	15	GPS99-06	20	Franco et al. (2012)
184	Block	282.5	18.3	GPS98-11	15*	Benford et al. (2012)
185	Tainan	120.19	23	GPS/InSAR	4*	Huang et al. (2009)
186	Houchiali	120.24	23	GPS/InSAR	4*	Huang et al. (2009)
187	Chungchou	120.26	23	GPS/InSAR	4.1*	Huang et al. (2009)

¹ Block: block model with constant locking depth; CJFS: Central Jamaica Fault System; DSF: Dead Sea fault; DV-FC: Death Valley-Furnace Creek; ETR: Eastern Transverse Ranges Province; EVZ: Eastern Volcanic Zone; GL: Grimsey Lineament; HFF: Husavik-Flatey Fault; JVF: Jordan Valley fault; KR: Kolbeinsey Ridge; LL-BW: Little Lake - Black Water Fault; MHT: Main Himalayan Thrust; MRF: Main Recent Fault; MZP: Zendan-Minab-Palami fault; NAF: North Anatolian Fault; NH: North Hispaniola; N. MMF: northern Marmara Fault; NTF: north Tabriz fault; NVZ: Northern Volcanic Zone; OV: Owens Valley; PMFS: Polochic-Motagua Fault System; PV-HM: Panamint Valley-Hunter Mountain; RP: Reykjanes Peninsula; RPW: Western Reykjanes Peninsula; RR: Reykjanes Ridge; SA: San Andreas; SB: San Bernardino; SISZ: South Iceland Seismic Zone; SJF: San Jacinto Fault; SJM: San Jacinto Mountain; SJV: San Jacinto Valley; SKJ: Sabzevaran-Kahnuj-Jirsoft fault; SM: Superstition Mountain; SP: Satellite-Pahrump; WAF: Wadi Araba fault; WVZ: Western Volcanic Zone; YM: Yucca Mountain; YZS: Yarlung-Zangbo Suture.

² *: Fixed locking depth

³ Corresponding to three profiles in the literature

⁴ For single and two faults models respectively

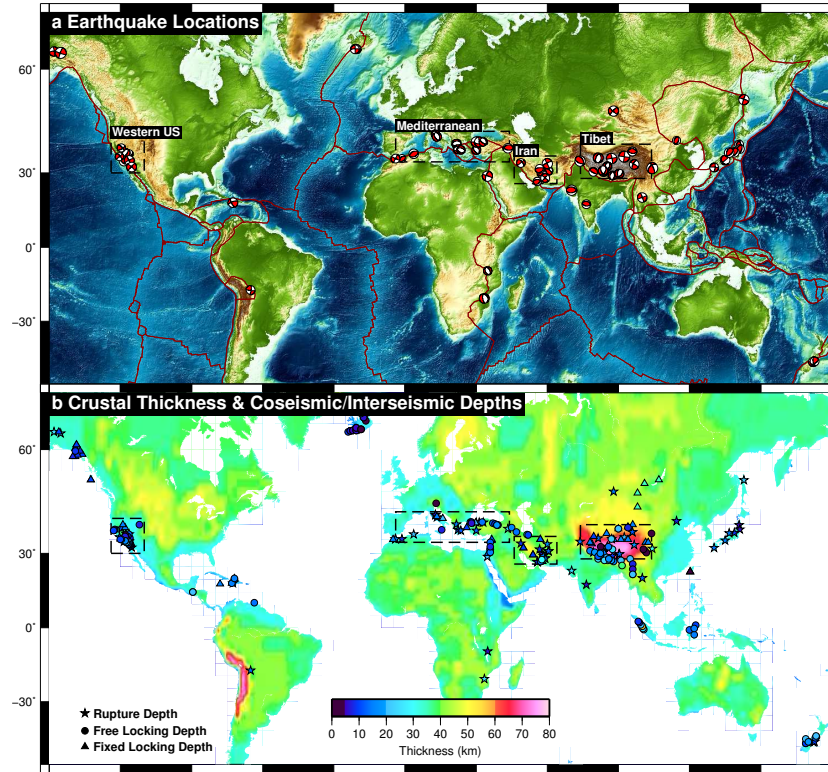


Figure 1: (a) Locations and focal mechanisms of the 78 continental M_w 5.5+ earthquakes modelled to date with InSAR observations of surface deformation, updated from Weston et al. (2011, 2012) and listed in Tables 1–3. The areas of four continental regions used to subdivide the plots in Figure 5 are delineated by dashed lines. (b) Crustal thickness from Crust 2.0 (Bassin et al., 2000), linearly interpolated to one degree spacing. Coloured stars indicate the bottom depth of faulting from coseismic studies (Tables 1–3). Locations of interseismic studies listed in Table 4 are coloured by depth and denoted by triangles (fixed locking depths) and circles (estimated locking depths).

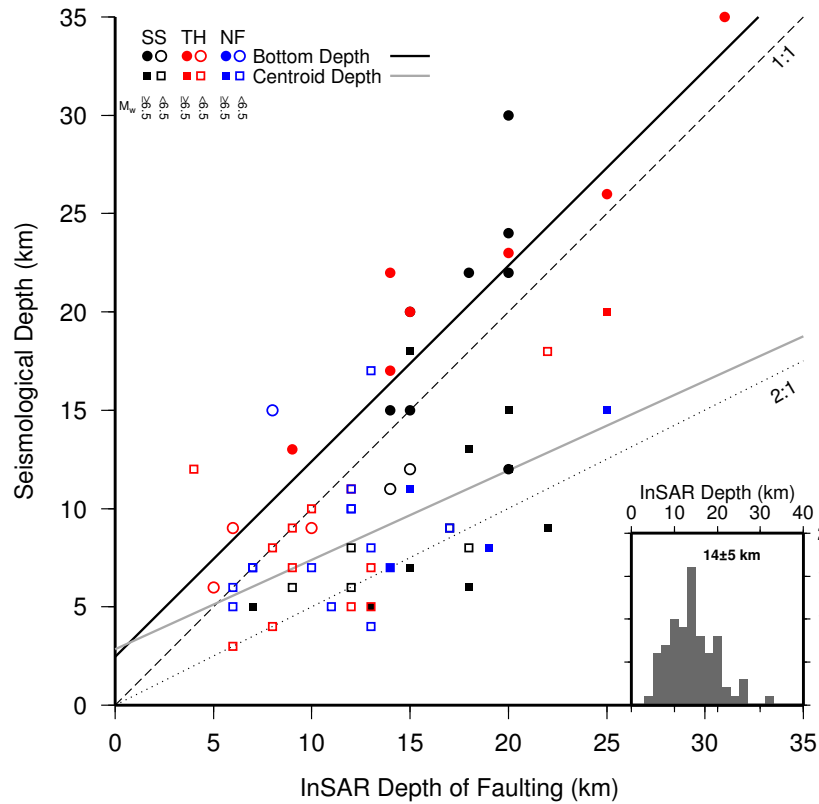


Figure 2: Correlation between InSAR derived bottom depths of faulting given in Tables 1–3 and seismological depths from centroid estimates (squares) or bottom of distributed sources (circles). Events are coloured by mechanism: reverse (red), strike-slip (black) and normal faulting (blue). Open symbols denoted $M_w < 6.5$, filled $M_w > 6.5$. The black line is the linear regression of the InSAR depths against the seismological bottom estimates, whilst the grey line is for the seismological centroid estimates. Inset figure shows the distribution of 78 InSAR derived bottom fault depths.

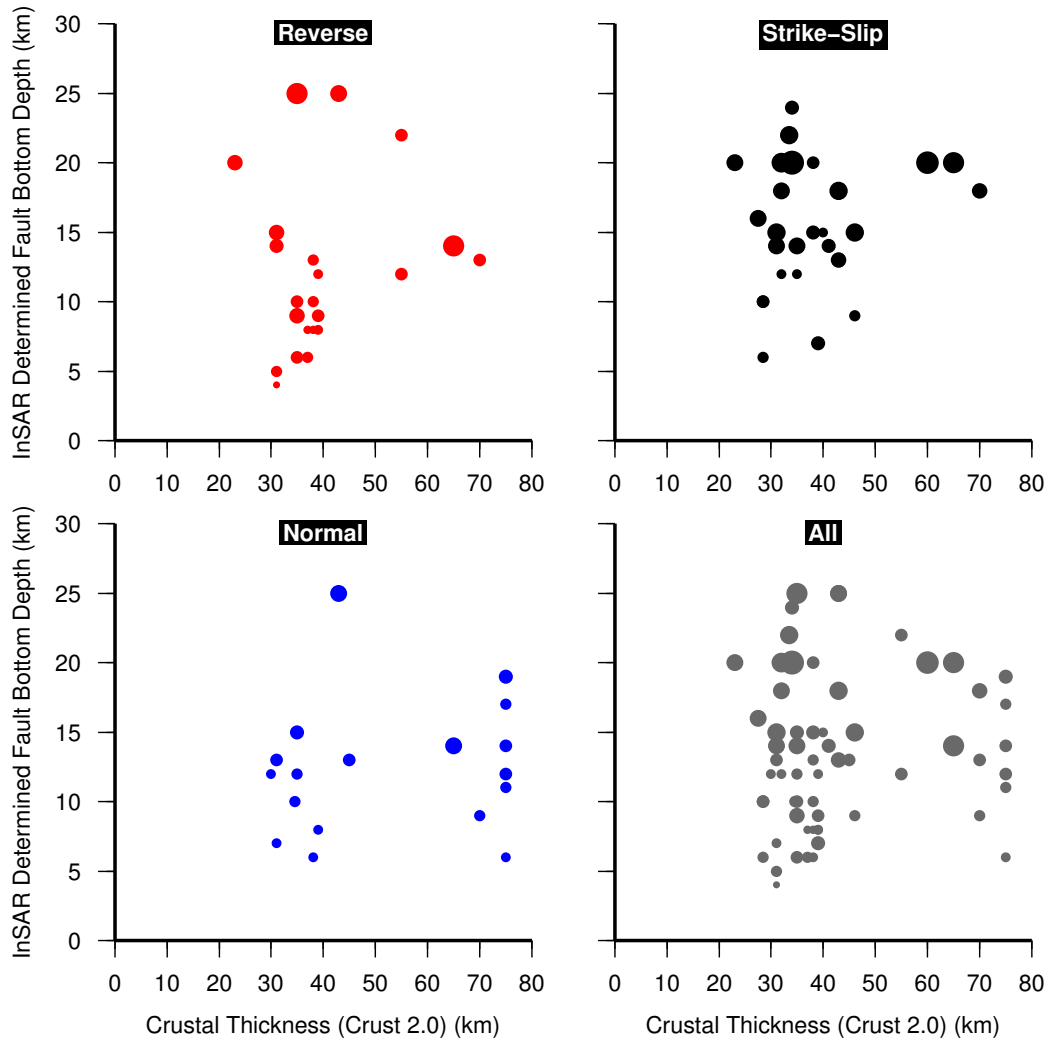


Figure 3: Correlation between InSAR derived bottom depths of faulting given in Tables 1–3 and Crust 2.0 thickness (Bassin et al., 2000) for reverse (red), strike-slip (black), normal faulting (blue) and all events combined (grey), scaled by magnitude (M_w 5.5–7.8).

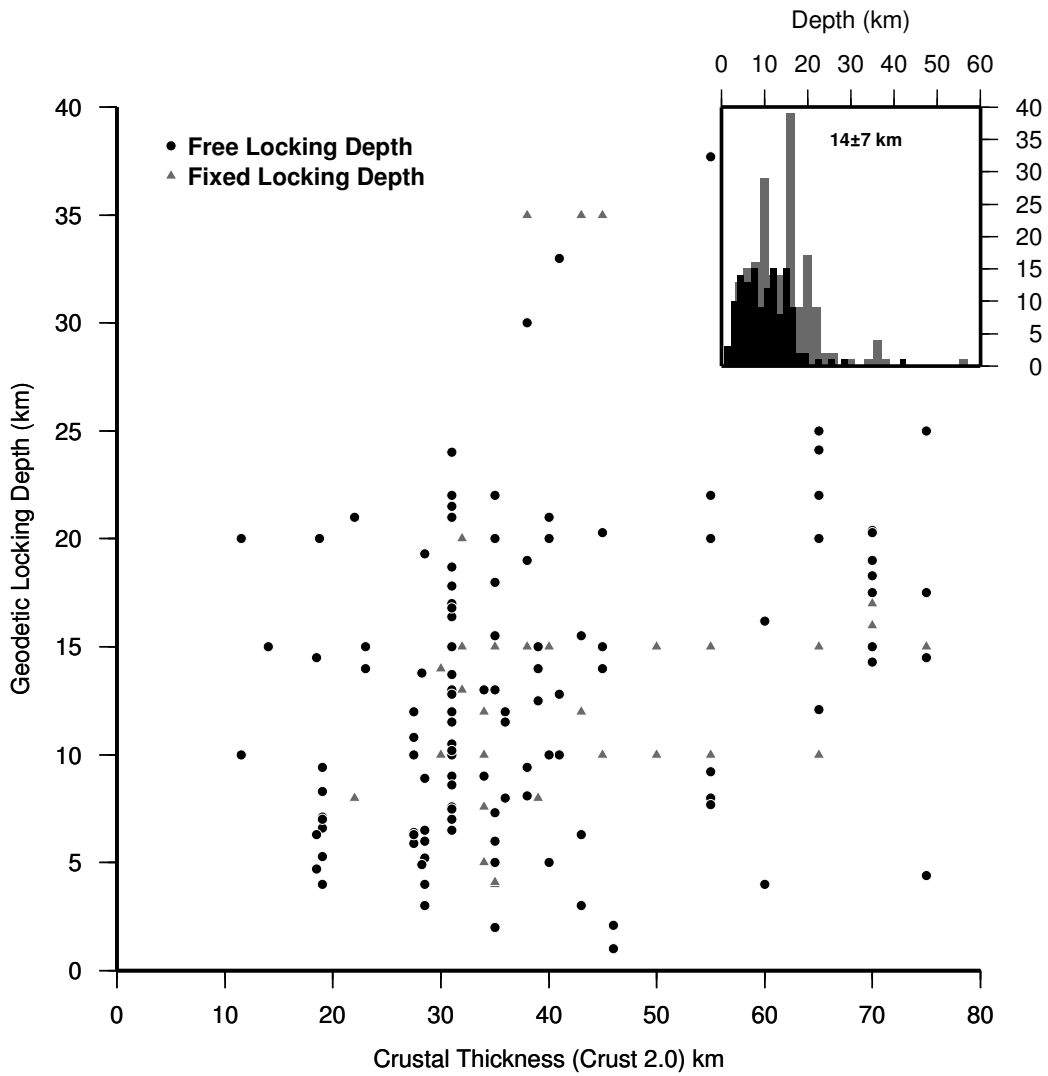


Figure 4: Correlation between interseismic locking depth (Table 4) and Crust 2.0 thickness (Bassin et al., 2000). Symbols indicate whether the locking depth was fixed (triangles) or free to vary (circles) in the respective study. Inset figure shows the distribution of 187 geodetically derived locking depths separated by free (black) and fixed (grey).

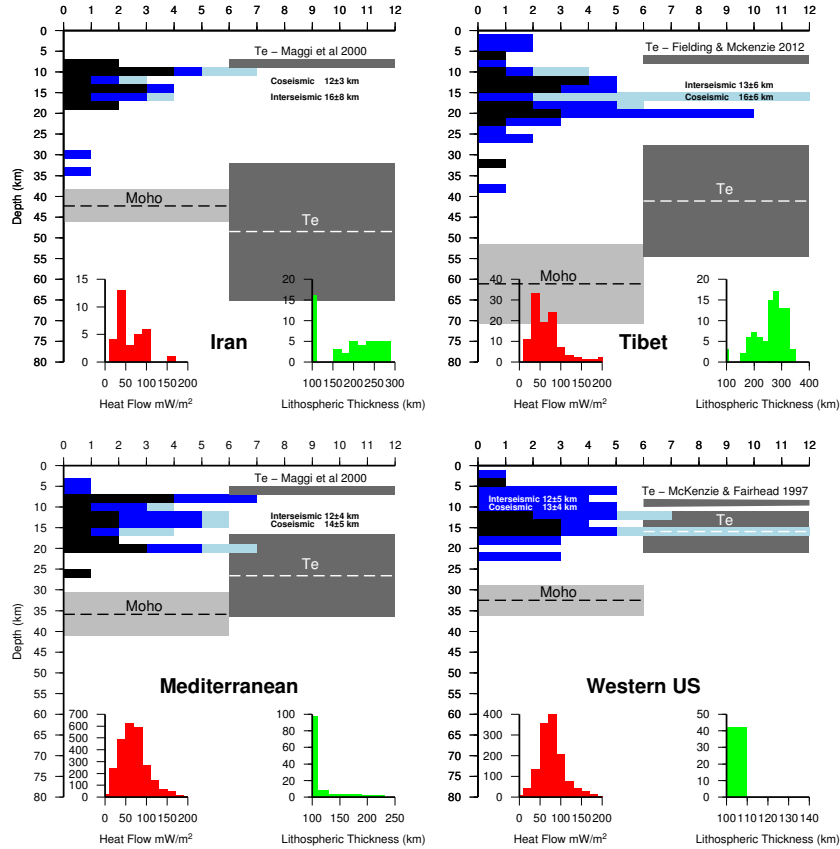


Figure 5: Histograms of earthquake rupture bottom depths (black bars) determined from InSAR-constrained coseismic slip models based upon the data in Tables 1–3, grouped by four continental regions shown in Figure 1. Blue bars are from the locking depths of interseismic studies shown in Table 4, for fixed (light-blue) and estimated depths (dark-blue). The mean (dashed line) Moho depths (Figure 1b) and one standard deviation (light grey panel) within each region are from the CRUST2.0 model (Bassin et al., 2000). The mean (dashed white line) elastic thicknesses (T_e) from Audet and Bürgmann (2011) and one standard deviation (dark grey panel) within each region are also shown. Elastic thicknesses from individual studies using free-air gravity are also shown from McKenzie and Fairhead (1997); Maggi et al. (2000); Fielding and McKenzie (2012). The inset red histograms show the distribution of heat flow within the region from the database updated by Hasterok and Chapman (2008). The inset green histograms show the distribution of lithospheric thickness within the region from Priestley and McKenzie (2006). Note the method used by Priestley and McKenzie (2006) cannot resolve lithospheric thicknesses less than 100 km.

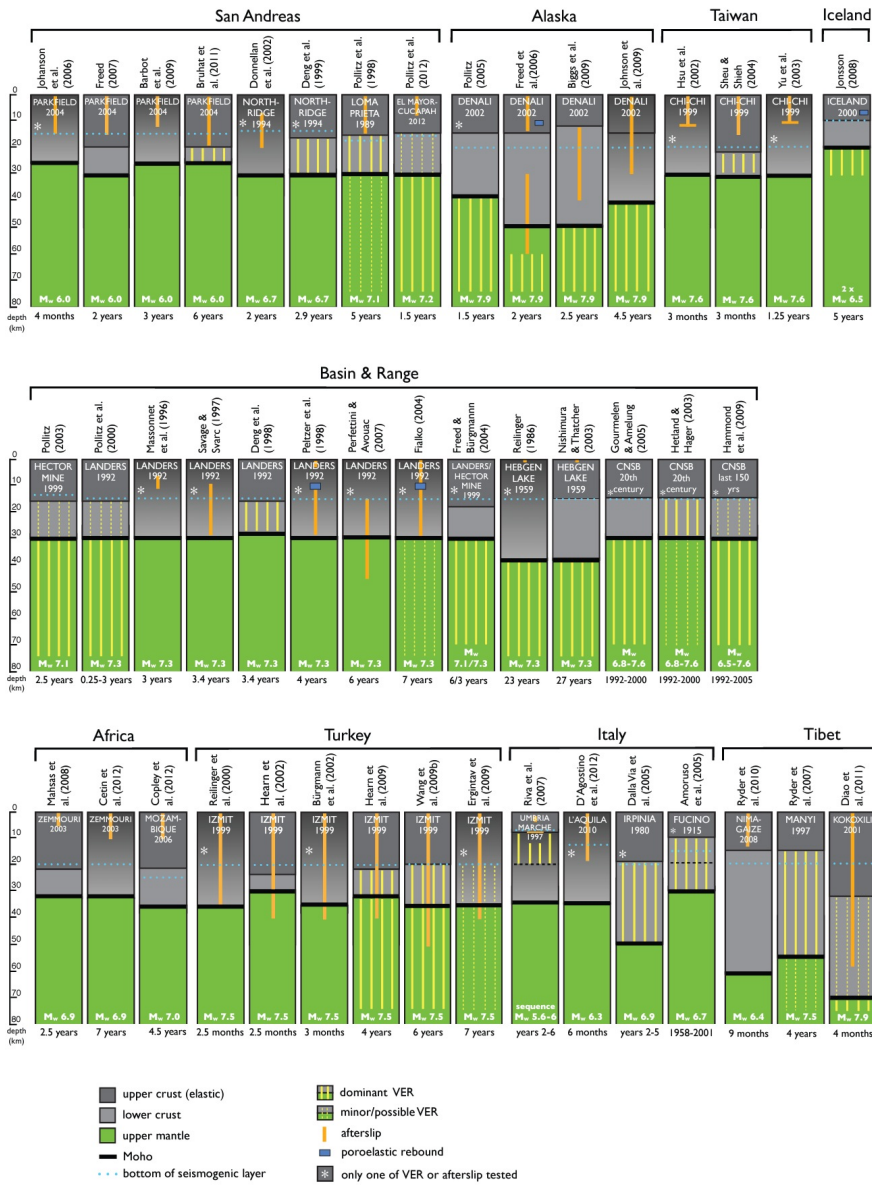


Figure 6: Global compilation of rheological interpretations of postseismic geodetic data. VER = viscoelastic relaxation. Each column represents a single case study, either for an individual earthquake or a group of earthquakes. Grey background denotes crust and green background denotes mantle. Where the crust is divided into upper and lower layers, upper crustal thickness is either assumed to be the maximum rupture depth/seismogenic thickness for the area, or is directly estimated from the geodetic data. The magnitude of each earthquake is given at the bottom of each column (white text), along with the geodetic observation period (black text). A white asterisk means that the study only investigated a single relaxation process (either afterslip or viscoelastic relaxation). Minor/possible VER implies that viscosities for a particular layer are poorly-constrained, and/or are within one order of magnitude greater than for the layer where dominant VER occurs. Seismogenic thickness is marked for reference (light blue dotted lines)

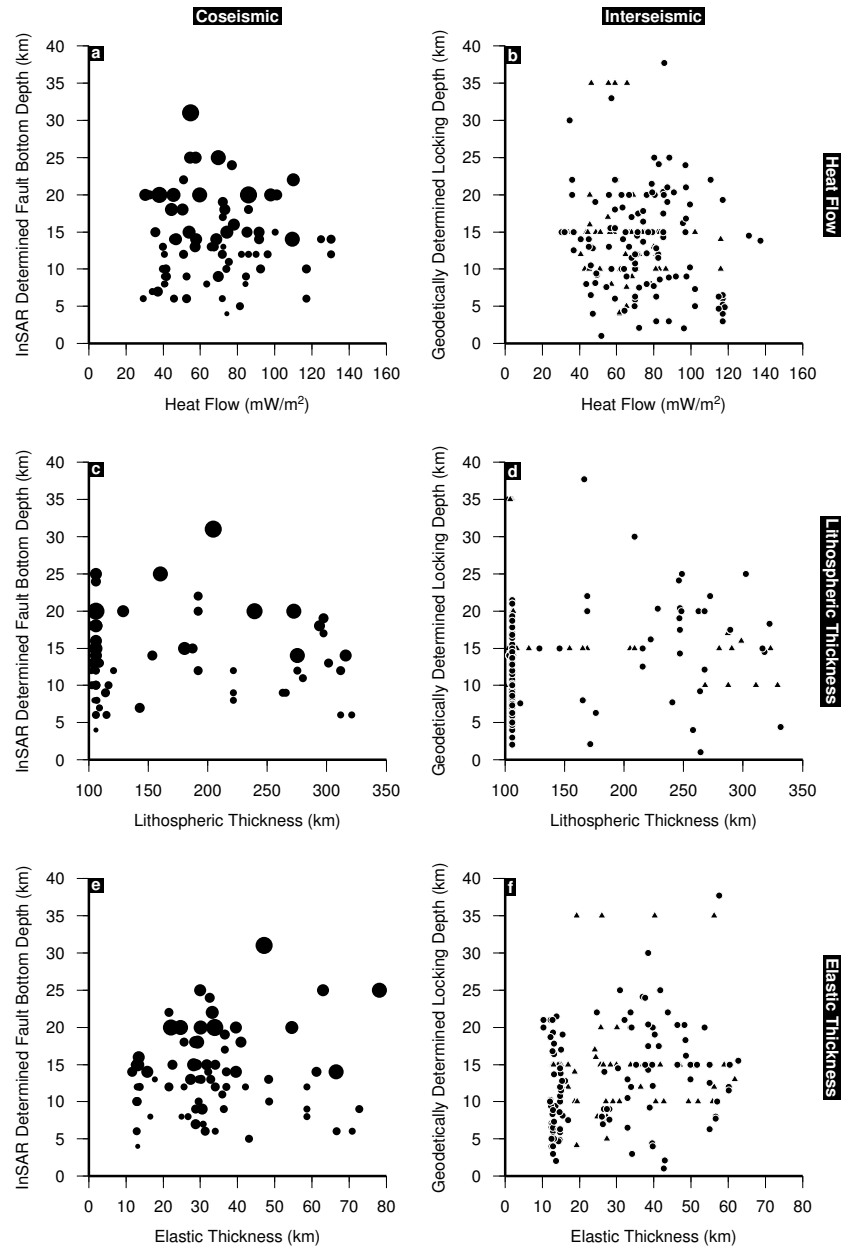


Figure 7: Correlation between InSAR-derived bottom depths of faulting given in Tables 1–3, or geodetically-determined locking depths given in Table 4, and elastic thickness (T_e) (Audet and Bürgmann, 2011), lithospheric thickness (Priestley and McKenzie, 2006) and heat flow (Hasterok and Chapman, 2008). The method used by Priestley and McKenzie (2006) cannot resolve lithospheric thicknesses less than 100 km. Coseismic events are scaled by magnitude (M_w 5.5–7.8); interseismic locking depths are plotted as circles if they were determined by free inversion, or triangles if they were held fixed.

567 **References**

568 Ader, T., Avouac, J.P., Liu-Zeng, J., et al., 2012. Convergence rate across
569 the Nepal Himalaya and interseismic coupling on the Main Himalayan
570 Thrust: Implications for seismic hazard. *Journal of Geophysical Research*
571 117, B04403, doi:10.1029/2011JB009071.

572 Ágústsson, K., Flóvenz, Ó.G., 2005. The thickness of the seismogenic crust
573 in Iceland and its implications for geothermal systems, in: *Proceedings of*
574 *the World Geothermal Congress*, pp. 24–29.

575 Amelung, F., Bell, J.W., 2003. Interferometric synthetic aperture radar ob-
576 servations of the 1994 Double Spring Flat, Nevada, earthquake (M5.9):
577 Main shock accompanied by triggered slip on a conjugate fault. *Journal*
578 *of Geophysical Research* 108.

579 Amoruso, A., Crescentini, L., D’Anastasio, E., De Martini, P., 2005. Clues
580 of postseismic relaxation for the 1915 Fucino earthquake (central Italy)
581 from modeling of leveling data. *Geophysical Research Letters* 32, L22307,
582 doi:10.1029/2005GL024139.

583 Antolik, M., Abercrombie, R.E., Ekstrom, G., 2004. The 14 November 2001
584 Kokoxili (Kunlunshan), Tibet, Earthquake: Rupture Transfer through a
585 Large Extensional Step-Over. *The Bulletin of the Seismological Society of*
586 *America* 94, 1173–1194.

587 Antolik, M., Dreger, D.S., 2003. Rupture Process of the 26 January
588 2001 Mw 7.6 Bhuj, India, Earthquake from Teleseismic Broadband

589 Data. Bulletin of the Seismological Society of America 93, 1235–1248.
590 <http://www.bssaonline.org/cgi/reprint/93/3/1235.pdf>.

591 Árnadóttir, T., Jiang, W., Feigl, K.L., et al., 2006. Kinematic mod-
592 els of plate boundary deformation in southwest Iceland derived from
593 GPS observations. Journal of Geophysical Research 111, B07402,
594 doi:10.1029/2005JB003907.

595 Árnadóttir, T., Lund, B., Jiang, W., et al., 2009. Glacial rebound and plate
596 spreading: results from the first countrywide GPS observations in Iceland.
597 Geophysical Journal International 177, 691–716.

598 Asano, K., Iwata, T., 2009. Source Rupture Process of the 2004 Chuetsu,
599 Mid-Niigata Prefecture, Japan, Earthquake Inferred from Waveform Inver-
600 sion with Dense Strong-Motion Data. Bulletin of the Seismological Society
601 of America 99, 123–140.

602 Atzori, S., Antonioli, A., 2011. Optimal fault resolution in geodetic inversion
603 of coseismic data. Geophysics Journal International 185, 529–538.

604 Audet, P., Bürgmann, R., 2011. Dominant role of tectonic inheritance in
605 supercontinent cycles. Nature Geoscience 4, 184–187.

606 Avouac, J.P., Ayoub, F., Leprince, S., Konca, O., Helmberger, D.V., 2006.
607 The 2005, M_w 7.6 Kashmir earthquake: Sub-pixel correlation of ASTER
608 images and seismic waveforms analysis. Earth and Planetary Science Let-
609 ters 249, 514–528.

610 Baer, G., Funning, G.J., Shamir, G., Wright, T.J., 2008. The 1995 November

- 611 22, M_w 7.2 Gulf of Elat earthquake cycle revisited. *Geophysics Journal*
612 *International* 175, 1040–1054.
- 613 Banerjee, P., Bürgmann, R., 2002. Convergence across the northwest
614 Himalaya from GPS measurements. *Geophysical Research Letters* 29,
615 doi:10.1029/2002GL015184.
- 616 Banerjee, P., Bürgmann, R., Nagarajan, B., Apel, E., 2008. Intraplate de-
617 formation of the Indian subcontinent. *Geophysical Research Letters* 35,
618 L09605, doi:10.1029/2004GL019723.
- 619 Bassin, C., Laske, G., Masters, G., 2000. The Current Limits of Resolution
620 for Surface Wave Tomography in North America. *EOS Transactions AGU*
621 81, S12A–03.
- 622 Battaglia, M., Murray, M.H., Serpelloni, E., Bürgmann, R., 2004.
623 The Adriatic region: An independent microplate within the Africa-
624 Eurasia collision zone. *Geophysical Research Letters* 31, L18301,
625 doi:10.1029/2008GL035468.
- 626 Bayer, R., Chery, J., Tatar, M., et al., 2006. Active deformation in Zagros-
627 Makran transition zone inferred from GPS measurements. *Geophysical*
628 *Journal International* 165, 373–381.
- 629 Beavan, J., Denys, P., Denham, M., et al., 2010. Distribution of present-
630 day vertical deformation across the Southern Alps, New Zealand, from
631 10 years of GPS data. *Geophysical Research Letters* 37, L16305,
632 doi:10.1029/2010GL044165.

- 633 Beavan, J., Moore, M.A., Pearson, C.H., et al., 1999. Crustal deformation
634 during 1994-1998 due to oblique continental collision in the central South-
635 ern Alps, New Zealand, and implications for seismic potential of the Alpine
636 fault. *Journal of Geophysical Research* 104, 25233–25255.
- 637 Belabbès, S., Meghraoui, M., Çakir, Z., Bouhadad, Y., 2009a. InSAR anal-
638 ysis of a blind thrust rupture and related active folding: the 1999 Ain
639 Temouchent earthquake (M_w 5.7, Algeria) case study. *Journal of Seismol-
640 ogy* 13, 421–432.
- 641 Belabbès, S., Wicks, C., Çakir, Z., Meghraoui, M., 2009b. Rupture pa-
642 rameters of the 2003 Zemmouri (M_w 6.8), Algeria, earthquake from joint
643 inversion of interferometric synthetic aperture radar, coastal uplift, and
644 GPS. *Journal of Geophysical Research* 114.
- 645 Bell, M.A., Elliott, J.R., Parsons, B.E., 2011. Interseismic strain accumula-
646 tion across the Manyi fault (Tibet) prior to the 1997 Mw 7.6 earthquake.
647 *Geophysical Research Letters* 38, L24302, doi:10.1029/2011GL049762.
- 648 Bendick, R., Bilham, R., Freymueller, J., et al., 2000. Geodetic evidence for
649 a low slip rate in the Altyn Tagh fault system. *Nature* 404, 69–72.
- 650 Benford, B., DeMets, C., Tikoff, B., et al., 2012. Seismic hazard along the
651 southern boundary of the Gônave microplate: block modelling of GPS ve-
652 locities from Jamaica and nearby islands, northern Caribbean. *Geophysical
653 Journal International* 190, 59–74.
- 654 Berberian, M., Jackson, J.A., Fielding, E., Parsons, B.E., Priestley, K., Qo-
655 rash, M., Talebian, M., Walker, R., Wright, T.J., Baker, C., 2001. The

- 656 1998 March 14 Fandoqa earthquake (M_w 6.6) in Kerman province, south-
657 east Iran: re-rupture of the 1981 Sirch earthquake fault, triggering of slip
658 on adjacent thrusts and the active tectonics of the Gowk fault zone. *Geo-*
659 *physics Journal International* 146, 371–398.
- 660 Berberian, M., Jackson, J.A., Qorashi, M., Khatib, M.M., Priestley, K.,
661 Talebian, M., Ghafuri-Ashtiani, M., 1999. The 1997 May 10 Zirkuh
662 (Qa’enat) earthquake (M_w 7.2): faulting along the Sistan suture zone of
663 eastern Iran. *Geophysics Journal International* 136, 671–694.
- 664 Berberian, M., Jackson, J.A., Qorashi, M., Talebian, M., Khatib, M., Priest-
665 ley, K., 2000. The 1994 Sefidabeh earthquakes in eastern Iran: blind
666 thrusting and bedding-plane slip on a growing anticline, and active tec-
667 tonics of the Sistan suture zone. *Geophysics Journal International* 142,
668 283–299.
- 669 Bernard, P., Briole, P., Meyer, B., Lyon-Caen, H., Gomez, J.M., Tiberi, C.,
670 Berge, C., R., C., Hatzfeld, D., Lachet, C., Lebrun, B., Deschamps, A.,
671 Courboulex, F., Larroque, C., Rigo, A., Massonnet, D., Papadimitriou, P.,
672 Kassaras, J., Diagourtas, D., Makropoulos, K., Veis, G., Papazisi, E., Mit-
673 sakaki, C., Karakostas, V., Papadimitriou, E., Papanastassiou, D., Chou-
674 liaras, M., Stavrakakis, G., 1997. The $M_s = 6.2$, June 15, 1995 Aigion
675 earthquake (Greece): evidence for low angle normal faulting in the Corinth
676 rift. *Journal of Seismology* 1, 131–150.
- 677 Bettinelli, P., Avouac, J.P., Flouzat, M., et al., 2006. Plate motion of In-
678 dia and interseismic strain in the Nepal Himalaya from GPS and DORIS
679 measurements. *Journal of Geodesy* 80, 567–589.

- 680 Biggs, J., Bergman, E., Emmerson, B., Funning, G.J., Jackson, J., Parsons,
681 B., Wright, T.J., 2006. Fault identification for buried strike-slip earth-
682 quakes using InSAR: The 1994 and 2004 Al Hoceima, Morocco earth-
683 quakes. *Geophysics Journal International* 166, 1347–1362.
- 684 Biggs, J., Burgmann, R., Freymueller, J., Lu, Z., Parsons, B., Ryder, I.,
685 Schmalzle, G., Wright, T., 2009. The postseismic response to the 2002
686 M 7.9 Denali Fault earthquake: constraints from InSAR 2003-2005. *Geo-
687 physical Journal International* 176, 353–367.
- 688 Biggs, J., Nissen, E., Craig, T., Jackson, J., Robinson, D.P., 2010. Breaking
689 up the hanging wall of a rift-border fault: The 2009 Karonga earthquakes,
690 Malawi. *Geophysical Research Letters* 37.
- 691 Biggs, J., Wright, T., Lu, Z., et al., 2007. Multi-interferogram method for
692 measuring interseismic deformation: Denali Fault, Alaska. *Geophysical
693 Journal International* 170, 1165–1179.
- 694 Bilham, R., Larson, K., Freymueller, J., et al., 1997. GPS measurements of
695 present-day convergence across the Nepal Himalaya. *Nature* 386, 61–64.
- 696 Björnsson, A., 2008. Temperature of the Icelandic crust: Inferred from elec-
697 trical conductivity, temperature surface gradient, and maximum depth of
698 earthquakes. *Tectonophysics* 447, 136–141.
- 699 Bruhat, L., Barbot, S., Avouac, J.P., 2011. Evidence for postseismic defor-
700 mation of the lower crust following the 2004 Mw6.0 Parkfield earthquake.
701 *Journal of Geophysical Research* 116, B08401, doi:10.1029/2010JB008073.

702 Burgmann, R., Ayhan, M.E., Fielding, E.J., Wright, T.J., McClusky, S.,
703 Aktug, B., Demir, C., Lenk, O., Turkezer, A., 2002. Deformation during
704 the 12 November 1999 Duzce, Turkey, Earthquake, from GPS and In-
705 SAR Data. *Bulletin of the Seismological Society of America* 92, 161–171.
706 <http://www.bssaonline.org/cgi/reprint/92/1/161.pdf>.

707 Bürgmann, R., Dresen, G., 2008. Rheology of the lower crust and upper
708 mantle: Evidence from rock mechanics, geodesy, and field observations.
709 *Annu. Rev. Earth Planet. Sci.* 36, 531–567.

710 Bürgmann, R., Ergintav, S., Segall, P., et al., 2002. Time-dependent dis-
711 tributed afterslip on and deep below the Izmit earthquake rupture. *Bulletin*
712 *of the Seismological Society of America* 92, 126–137.

713 Burov, E., 2010. The equivalent elastic thickness (T_e), seismicity and the
714 long-term rheology of continental lithosphere: Time to burn-out “crème
715 brûlée”: Insights from large-scale geodynamic modeling. *Tectonophysics*
716 484, 4–26.

717 Burov, E., Watts, A., et al., 2006. The long-term strength of continental
718 lithosphere: “jelly sandwich” or “crème brûlée”? *GSA Today* 16, 4.

719 Burov, E.B., Watts, A.B., 2006. The long-term strength of continental litho-
720 sphere: ‘jelly sandwich’ or ‘crème brûlée’? *GSA Today* 16, 4–10.

721 Çakir, Z., de Chabalier, J.B., Armijo, R., Meyer, B., Barka, A., Peltzer,
722 G., 2003. Coseismic and early post-seismic slip associated with the 1999
723 Izmit earthquake (Turkey), from SAR interferometry and tectonic field
724 observations. *Geophysics Journal International* 155, 93–110.

- 725 Cakir, Z., Akoglu, A.M., 2008. Synthetic aperture radar interferometry ob-
726 servations of the $M = 6.0$ Orta earthquake of 6 June 2000 (NW Turkey):
727 Reactivation of a listric fault. *Geochemistry, Geophysics, and Geosystems*
728 9.
- 729 Çakir, Z., Akoglu, A.M., Belabbes, S., et al., 2005. Creeping along the
730 Ismetpasa section of the North Anatolian fault (Western Turkey): Rate
731 and extent from InSAR. *Earth and Planetary Science Letters* 238, 225–
732 234.
- 733 Calais, E., Freed, A., Mattioli, G., Amelung, F., Jónsson, S., Jansma, P.,
734 Hong, S.H., Dixon, T., Prépetit, C., Momplaisir, R., 2010. Transpressional
735 rupture of an unmapped fault during the 2010 Haiti earthquake. *Nature*
736 *Geoscience* 3, 794–799.
- 737 Calais, E., Mazabraud, Y., Mercier de Lépinay, B., et al., 2002.
738 Strain partitioning and fault slip rates in the northeastern Caribbean
739 from GPS measurements. *Geophysical Research Letters* 29, 1856,
740 doi:10.1029/2002GL015397.
- 741 Calais, E., Vergnolle, M., Sankov, V., et al., 2003. GPS measurements of
742 crustal deformation in the Baikal-Mongolia area (1994-2002): Implications
743 for current kinematics of Asia. *Journal of Geophysical Research* 108, B10,
744 2501, doi:10.1029/2002JB002373.
- 745 Cavalie, O., Lasserre, C., Doin, M.P., Peltzer, G., Sun, J., Xu, X., Shen,
746 Z.K., 2008. Measurement of interseismic strain across the Haiyuan fault

747 (Gansu, China), by InSAR. *Earth and Planetary Science Letters* 275, 246
748 – 257.

749 Cetin, E., Meghraoui, M., Cakir, Z., et al., 2012. Seven years of postseismic
750 deformation following the 2003 Mw = 6.8 Zemmouri earthquake (Alge-
751 ria) from InSAR time series. *Geophysical Research Letters* 39, L10307,
752 doi:10.1029/2012GL051344.

753 Chen, Q., Freymueller, J.T., Yang, Z., et al., 2004. Spatially variable exten-
754 sion in southern Tibet based on GPS measurements. *Journal of Geophys-
755 ical Research* 109, B09401, doi:10.1029/2002JB002350.

756 Cirella, A., Piatanesi, A., Cocco, M., Tinti, E., Scognamiglio, L., Michelini,
757 A., Lomax, A., Boschi, E., 2009. Rupture history of the 2009 L’Aquila
758 (Italy) earthquake from non-linear joint inversion of strong motion and
759 GPS data. *Geophysical Research Letters* 36.

760 Copley, A., Hollingsworth, J., Bergman, E., 2012. Constraints on fault and
761 lithosphere rheology from the coseismic slip and postseismic afterslip of
762 the 2006 Mw7.0 Mozambique earthquake. *Journal of Geophysical Research*
763 117.

764 Crosby, A., 2007. An assessment of the accuracy of admittance and coherence
765 estimates using synthetic data. *Geophysical Journal International* 171, 25–
766 54.

767 D’Agostino, N., Cheloni, D., Fornaro, G., Giuliani, R., Reale, D., 2012.
768 Space-time distribution of afterslip following the 2009 L’Aquila earthquake.
769 *Journal of Geophysical Research* 117, B02402, doi:10.1029/2011JB008523.

- 770 D’Agostino, N., Cheloni, D., Mantenuto, S., et al., 2005. Strain accumula-
771 tion in the southern Alps (NE Italy) and deformation at the northeastern
772 boundary of Adria observed by CGPS measurements. *Geophysical Re-*
773 *search Letters* 32, L19306, doi:10.1029/2005GL024266.
- 774 D’Agostino, N., Mantenuto, S., D’Anastasio, E., et al., 2011. Evidence for
775 localized active extension in the central Apennines (Italy) from global po-
776 sitioning system observations. *Geology* 39, 291–294.
- 777 Dalla Via, G., Sabadini, R., De Natale, G., Pingue, F., 2005. Lithospheric
778 rheology in southern Italy inferred from postseismic viscoelastic relaxation
779 following the 1980 Irpinia earthquake. *Journal of Geophysical Research*
780 110, B06311, doi:10.1029/2004JB003539.
- 781 Decriem, J., Árnadóttir, T., Hooper, A., Geirsson, H., Sigmundsson, F.,
782 Keiding, M., Ófeigsson, B.G., Hreinsdóttir, S., Einarsson, P., Lafemina,
783 P., Bennett, R.A., 2010. The 2008 May 29 earthquake doublet in SW
784 Iceland. *Geophysics Journal International* 181, 1128–1146.
- 785 Deng, J., Gurnis, M., Kanamori, H., et al., 1998. Viscoelastic flow in the
786 lower crust after the 1992 Landers, California, Earthquake. *Science* 282,
787 1689–1693.
- 788 Deng, J., Hudnut, K., Gurnis, M., Hauksson, E., 1999. Stress loading from
789 viscous flow in the lower crust and triggering of aftershocks following the
790 1994 Northridge, California, Earthquake. *Geophysical Research Letters*
791 26, 32093212.

- 792 Diao, F., Xiong, X., Wang, R., 2011. Mechanisms of Transient Postseismic
793 Deformation Following the 2001 Mw 7.8 Kunlun (China) Earthquake. *Pure
794 and Applied Geophysics* 168, 767–779.
- 795 Dixon, T.H., Farina, F., DeMets, C., et al., 1998. Relative motion between
796 the Caribbean and North American plates and related boundary zone de-
797 formation from a decade of GPS observations. *Journal of Geophysical
798 Research* 103, 15,157–15,182.
- 799 Djamour, Y., Vernant, P., Bayer, R., et al., 2010. GPS and gravity con-
800 straints on continental deformation in the Alborz mountain range, Iran.
801 *Geophysical Journal International* 183, 1287–1301.
- 802 Djamour, Y., Vernant, P., Nankali, H.R., et al., 2011. NW Iran-eastern
803 Turkey present-day kinematics: Results from the Iranian permanent GPS
804 network. *Earth and Planetary Science Letters* 307, 27–34.
- 805 Donnellan, A., Parker, J.W., Peltzer, G., 2002. Combined GPS and InSAR
806 models of postseismic deformation from the Northridge earthquake. *Pure
807 and Applied Geophysics* 159, 2261–2270.
- 808 Dreger, D.S., 1994. Empirical Green’s function study of the January 17,
809 1994 Northridge, California earthquake. *Geophysical Research Letters* 21,
810 2633–2636.
- 811 Elliott, J., Copley, A., Holley, R., Scharer, K., Parsons, B., 2013. The 2011
812 Mw 7.1 Van (Eastern Turkey) Earthquake. *Journal of Geophysical Re-
813 search* 118.

- 814 Elliott, J.L., Larsen, C.F., Freymueller, J.T., Motyka, R.J., 2010b. Tectonic
815 block motion and glacial isostatic adjustment in southeast Alaska and ad-
816 jacent Canada constrained by GPS measurements. *Journal of Geophysical*
817 *Research* 115, B09407, doi:10.1029/2009JB007139.
- 818 Elliott, J.R., Biggs, J., Parsons, B., et al., 2008. InSAR slip rate determi-
819 nation on the Altyn Tagh Fault, northern Tibet, in the presence of topo-
820 graphically correlated atmospheric delays. *Geophysical Research Letters*
821 35, L12309, doi:10.1029/2008GL033659.
- 822 Elliott, J.R., Nissen, E.K., England, P.C., Jackson, J.A., Lamb, S., Li, Z.,
823 Oehlers, M., Parsons, B., 2012. Slip in the 2010–2013 Canterbury
824 earthquakes, New Zealand. *Journal of Geophysical Research* 117.
- 825 Elliott, J.R., Parsons, B., Jackson, J.A., Shan, X., Sloan, R.A., Walker, R.T.,
826 2011. Depth segmentation of the seismogenic continental crust: The 2008
827 and 2009 Qaidam earthquakes. *Geophysical Research Letters* 38, L06305.
- 828 Elliott, J.R., Walters, R.J., England, P.C., Jackson, J.A., Li, Z., Parsons, B.,
829 2010. Extension on the Tibetan plateau: recent normal faulting measured
830 by InSAR and body wave seismology. *Geophysics Journal International*
831 183, 503–535.
- 832 Ergintav, S., McClusky, S., Hearn, E., et al., 2009. Seven years of postseismic
833 deformation following the 1999, M=7.4 and M=7.2, Izmit-Duzce, Turkey
834 earthquake sequence. *Journal of Geophysical Research* 114.
- 835 Feigl, K.L., Sargent, A., Jacq, D., 1995. Estimation of an earthquake focal
836 mechanism from a satellite radar interferogram: Application to the Decem-

837 ber 4, 1992 Landers aftershock. *Geophysical Research Letters* 22, 1037–
838 1040.

839 Feng, W., Li, Z., Elliott, J.R., Fukushima, Y., Hoey, T., Singleton, A., Cook,
840 R., Xu, Z., 2013. The 2011 Mw 6.8 Burma earthquake: Fault constraints
841 provided by multiple SAR techniques. *Geophysics Journal International* .

842 Fialko, Y., 2004. Evidence of fluid-filled upper crust from observations of
843 postseismic deformation due to the 1992 Mw7. 3 Landers earthquake. *Jour-
844 nal of Geophysical Research* 109, B03307, doi:10.1029/2003JB002985.

845 Fialko, Y., 2004. Probing the mechanical properties of seismically active crust
846 with space geodesy: Study of the coseismic deformation due to the 1992
847 M_w 7.3 Landers (southern California) earthquake. *Journal of Geophysical
848 Research* 109, B03307.

849 Fialko, Y., 2006. Interseismic strain accumulation and the earthquake po-
850 tential on the southern San Andreas fault system. *Nature* 441, 968–971.

851 Fielding, E., McKenzie, D., 2012. Lithospheric flexure in the sichuan basin
852 and longmen shan at the eastern edge of tibet. *Geophysical Research
853 Letters* 39, L09311.

854 Fletcher, H.J., Freymueller, J.T., 2003. New constraints on the motion of the
855 Fairweather fault, Alaska, from GPS observations. *Geophysical Research
856 Letters* 30, 1139, doi:10.1029/2002GL016476.

857 Floyd, M., Billiris, H., Paradissis, D., Veis, G., Avallone, A., Briole, P.,
858 McClusky, S., Nocquet, J., Palamartchouk, K., Parsons, B., et al., 2010. A

- 859 new velocity field for Greece: Implications for the kinematics and dynamics
860 of the Aegean. *J. Geophys. Res* 115, B10403.
- 861 Forsyth, D., 1985. Subsurface loading and estimates of the flexural rigidity
862 of continental lithosphere. *Journal of Geophysical Research* 90, 12623–12.
- 863 Franco, A., Lasserre, C., Lyon-Caen, H., et al., 2012. Fault kinematics in
864 northern Central America and coupling along the subduction interface of
865 the Cocos Plate, from GPS data in Chiapas (Mexico), Guatemala and El
866 Salvador. *Geophysical Journal International* 189, 1223–1236.
- 867 Freed, A., Bürgmann, R., 2004. Evidence of power-law flow in the Mojave
868 desert mantle. *Nature* 430, 548–551.
- 869 Freed, A., Bürgmann, R., Calais, E., Freymueller, J., Hreinsdóttir, S., 2006.
870 Implications of deformation following the 2002 Denali, Alaska, earthquake
871 for postseismic relaxation processes and lithospheric rheology. *Journal of*
872 *Geophysical Research* 111, B01401.
- 873 Freed, A.M., 2007. Afterslip (and only afterslip) following the 2004 Park-
874 field, California, earthquake. *Geophysical Research Letters* 34, L06312,
875 doi:10.1029/2006GL029155.
- 876 Fujiwara, S., Rosen, P.A., Tobita, M., Murakami, M., 1998. Crustal defor-
877 mation measurements using repeat-pass JERS 1 synthetic aperture radar
878 interferometry near the Izu Peninsula, Japan. *Journal of Geophysical Re-*
879 *search* 103, 2411–2426.
- 880 Fukushima, Y., Ozawa, T., Hashimoto, M., 2008. Fault model of the 2007

- 881 Noto Hanto earthquake estimated from PALSAR radar interferometry and
882 GPS data. *Earth, Planets, and Space* 60, 99–104.
- 883 Funning, G.J., 2005. Source parameters of large shallow earthquakes in the
884 Alpine-Himalayan belt from InSAR and waveform modelling. Ph.D. thesis.
885 Department of Earth Sciences, University of Oxford. Oxford, U.K.
- 886 Funning, G.J., Barke, R.M.D., Lamb, S.H., Minaya, E., Parsons, B., Wright,
887 T.J., 2005a. The 1998 Aiquile, Bolivia earthquake: A seismically active
888 fault revealed with InSAR. *Earth and Planetary Science Letters* 232, 39–
889 49.
- 890 Funning, G.J., Parsons, B., Wright, T.J., 2007. Fault slip in the 1997 Manyi,
891 Tibet earthquake from linear elastic modelling of InSAR displacements.
892 *Geophysics Journal International* 169, 988–1008.
- 893 Funning, G.J., Parsons, B., Wright, T.J., Jackson, J.A., Fielding, E.J., 2005b.
894 Surface displacements and source parameters of the 2003 Bam (Iran) earth-
895 quake from Envisat advanced synthetic aperture radar imagery. *Journal*
896 *of Geophysical Research* 110, B09406.
- 897 Gan, W., Svarc, J.L., Savage, J.C., Prescott, W.H., 2000. Strain accumula-
898 tion across the Eastern California Shear Zone at latitude 36°30'N. *Journal*
899 *of Geophysical Research* 105, 16,229–16,236.
- 900 Genrich, J., Bock, Y., McCaffrey, R., et al., 2000. Distribution of slip at the
901 northern Sumatran fault system. *Journal of Geophysical Research* 105,
902 28327–28341.

- 903 Gomez, F., Karam, G., Khawlie, M., et al., 2007. Global Positioning Sys-
904 tem measurements of strain accumulation and slip transfer through the
905 restraining bend along the Dead Sea fault system in Lebanon. *Geophysical*
906 *Journal International* 168, 1021–1028.
- 907 Gourmelen, N., Amelung, F., 2005. Postseismic mantle relaxation in the
908 central Nevada seismic belt. *Science* 310, 1473–1476.
- 909 Gourmelen, N., Amelung, F., Lanari, R., 2010. Interferometric synthetic
910 aperture radarGPS integration: Interseismic strain accumulation across
911 the Hunter Mountain fault in the eastern California shear zone. *Journal*
912 *of Geophysical Research* 115, B09408, doi:10.1029/2009JB007064.
- 913 Hammond, W., Blewitt, G., Kreemer, C., 2011. Block modeling of crustal
914 deformation of the northern Walker Lane and Basin and Range from GPS
915 velocities. *Journal of Geophysical Research* 116, B04402.
- 916 Hammond, W.C., Blewitt, G., Kreemer, C., 2011. Block modeling of
917 crustal deformation of the northern Walker Lane and Basin and Range
918 from GPS velocities. *Journal of Geophysical Research* 116, B04402,
919 doi:10.1029/2010JB007817.
- 920 Hammond, W.C., Kreemer, C., Blewitt, G., 2009. Geodetic constraints on
921 contemporary deformation in the northern Walker Lane: 3. Central Nevada
922 seismic belt postseismic relaxation, in: Oldow, J.S., Cashman, P.H. (Eds.),
923 *Late Cenozoic Structure and Evolution of the Great BasinSierra Nevada*
924 *Transition: Geological Society of America Special Paper*, pp. 33–54.

- 925 Hammond, W.C., Thatcher, W., 2007. Crustal deformation across the
926 Sierra Nevada, northern Walker Lane, Basin and Range transition, west-
927 ern United States measured with GPS, 20002004. *Journal of Geophysical*
928 *Research* 112, B05411, doi:10.1029/2006JB004625.
- 929 Hao, K.X., Si, H., Fujiwara, H., Ozawa, T., 2009. Coseismic surface-ruptures
930 and crustal deformations of the 2008 wenchuan earthquake mw7.9, china.
931 *Geophysical Research Letters* 36.
- 932 Hasterok, D., Chapman, D.S., 2008. Global Heat Flow: A New Database
933 and a New Approach, in: AGU Fall Meeting Abstracts.
- 934 Hatzfeld, D., Karakostas, V., Ziazia, M., Selvaggi, G., Leborgne, S., Berge,
935 C., Guiguet, R., Paul, A., Voidomatis, P., Diagnourtas, D., Kassaras,
936 I., Koutsikos, I., Makropoulos, K., Azzara, R., Di Bona, M., Bacch-
937 eschi, S., Bernard, P., Papaioannou, C., 1997. The Kozani-Grevena
938 (Greece) earthquake of 13 May 1995 revisited from a detailed seismolog-
939 ical study. *Bulletin of the Seismological Society of America* 87, 463–473.
940 <http://www.bssaonline.org/cgi/reprint/87/2/463.pdf>.
- 941 Hayes, G.P., Briggs, R.W., Sladen, A., Fielding, E.J., Prentice, C., Hudnut,
942 K., Mann, P., Taylor, F.W., Crone, A.J., Gold, R., Ito, T., Simons, M.,
943 2010. Complex rupture during the 12 January 2010 Haiti earthquake.
944 *Nature Geoscience* 3, 800–805.
- 945 Hearn, E., Bürgmann, R., Reilinger, R., 2002. Dynamics of Izmit earthquake
946 postseismic deformation and loading of the Duzce earthquake hypocenter.
947 *Bulletin of the Seismological Society of America* 92, 172–193.

- 948 Hearn, E.H., McClusky, S., Ergintav, S., Reilinger, R.E., 2009. Izmit
949 earthquake postseismic deformation and dynamics of the North Ana-
950 tolian Fault Zone. *Journal of Geophysical Research* 114, B08405,
951 doi:10.1029/2008JB006026.
- 952 Hernandez, B., Cocco, M., Cotton, F., Stramondo, S., Scotti, O., Cour-
953 boulex, F., Campillo, M., 2004. Rupture history of the 1997 Umbria-
954 Marche (Central Italy) main shocks from the inversion of GPS, DInSAR
955 and near field strong motion data. *Annals of Geophysics* 47, 1355–1376.
- 956 Hetland, E., Hager, B., 2003. Postseismic relaxation across the Cen-
957 tral Nevada Seismic Belt. *Journal of Geophysical Research* 108, 2394,
958 doi:10.1029/2002JB002257.
- 959 Hetland, E., Hager, B., 2006. The effects of rheological layering on post-
960 seismic deformation. *Geophysical Journal International* 166, 277–292.
- 961 Hikima, K., Koketsu, K., 2004. Source processes of the foreshock, mainshock
962 and largest aftershock in the 2003 Miyagi-ken Hokubu, Japan, earthquake
963 sequence. *Earth, Planets, and Space* 56, 87–93.
- 964 Hill, E.M., Blewitt, G., 2006. Testing for fault activity at Yucca Moun-
965 tain, Nevada, using independent GPS results from the BARGEN network.
966 *Geophysical Research Letters* 33, L14302, doi:10.1029/2006GL026140.
- 967 Hofstetter, A., Thio, H.K., Shamir, G., 2003. Source mechanism of the
968 22/11/1995 Gulf of Aqaba earthquake and its aftershock sequence. *Journal*
969 *of Seismology* 7, 99–114.

- 970 Holden, C., 2011. Kinematic Source Model of the 22 February 2011 Mw
971 6.2 Christchurch Earthquake Using Strong Motion Data. *Seismological*
972 *Research Letters* , 783–788.
- 973 Horikawa, H., 2001. Earthquake Doublet in Kagoshima,
974 Japan: Rupture of Asperities in a Stress Shadow. *Bul-*
975 *letin of the Seismological Society of America* 91, 112–127.
976 <http://www.bssaonline.org/cgi/reprint/91/1/112.pdf>.
- 977 Horikawa, H., 2008. Characterization of the 2007 Noto Hanto, Japan, earth-
978 quake. *Earth, Planets, and Space* 60, 1017–1022.
- 979 Hsu, Y.J., Bechor, N., Segall, P., 2002. Rapid afterslip following the 1999
980 Chi-Chi, Taiwan Earthquake. *Geophysical Research Letters* 19, 1754,
981 doi:10.1029/2002GL014967.
- 982 Huang, M.H., Hu, J.C., Ching, K.E., et al., 2009. Active deformation of
983 Tainan tableland of southwestern Taiwan based on geodetic measurements
984 and SAR interferometry. *Tectonophysics* 466, 322 – 334.
- 985 Ichinose, G.A., Smith, K.D., Anderson, J.G., 1998. Moment ten-
986 sor solutions of the 1994 to 1996 Double Spring Flat, Nevada,
987 earthquake sequence and implications for local tectonic models.
988 *Bulletin of the Seismological Society of America* 88, 1363–1378.
989 <http://www.bssaonline.org/cgi/reprint/88/6/1363.pdf>.
- 990 Ide, S., Takeo, M., Yoshida, Y., 1996. Source process of the 1995 Kobe earth-
991 quake: Determination of spatio-temporal slip distribution by Bayesian

- 992 modeling. *Bulletin of the Seismological Society of America* 86, 547–566.
993 <http://www.bssaonline.org/cgi/reprint/86/3/547.pdf>.
- 994 Jackson, J., Bouchon, M., Fielding, E., Funning, G., Ghorashi, M., Hatzfeld,
995 D., Nazari, H., Parsons, B., Priestley, K., Talebian, M., Tatar, M., Walker,
996 R., Wright, T., 2006. Seismotectonic, rupture process, and earthquake-
997 hazard aspects of the 2003 December 26 Bam, Iran, earthquake. *Geo-
998 physics Journal International* 166, 1270–1292.
- 999 Jackson, J., McKenzie, D., Priestley, K., Emmerson, B., 2008. New views on
1000 the structure and rheology of the lithosphere. *Journal of the Geological
1001 Society* 165, 453–465.
- 1002 Jackson, J.A., 2002. Strength of the continental lithosphere: Time to aban-
1003 don the jelly sandwich? *GSA Today* 12, 4–10.
- 1004 Ji, C., Wald, D.J., Helmberger, D.V., 2002. Source Description of the 1999
1005 Hector Mine, California, Earthquake, Part II: Complexity of Slip History.
1006 *Bulletin of the Seismological Society of America* 92, 1208–1226.
- 1007 Johanson, I.A., Fielding, E.J., Rolandone, F., Burgmann, R., 2006. Coseis-
1008 mic and Postseismic Slip of the 2004 Parkfield Earthquake from Space-
1009 Geodetic Data. *Bulletin of the Seismological Society of America* 96, S269–
1010 282. <http://www.bssaonline.org/cgi/reprint/96/4B/S269.pdf>.
- 1011 Johnson, K., Hilley, G., Bürgmann, R., 2007a. Influence of lithosphere vis-
1012 cosity structure on estimates of fault slip rate in the Mojave region of the
1013 San Andreas fault system. *Journal of Geophysical Research* 112, B07408,
1014 doi:10.1029/2006JB004842.

- 1015 Johnson, K.M., Bürgmann, R., Freymueller, J.T., 2009. Coupled afterslip
1016 and viscoelastic flow following the 2002 Denali Fault, Alaska earthquake.
1017 *Geophysical Journal International* 176, 670–682.
- 1018 Johnson, K.M., Hilley, G.E., Bürgmann, R., 2007b. Influence of lithosphere
1019 viscosity structure on estimates of fault slip rate in the Mojave region of the
1020 San Andreas fault system. *Journal of Geophysical Research* 112, B07408,
1021 doi:10.1029/2006JB004842.
- 1022 Jolivet, R., Bürgmann, R., Houlié, N., 2009. Geodetic exploration of the
1023 elastic properties across and within the northern San Andreas Fault zone.
1024 *Earth and Planetary Science Letters* 288, 126–131.
- 1025 Jolivet, R., Cattin, R., Chamot-Rooke, N., et al., 2008. Thin-plate
1026 modeling of interseismic deformation and asymmetry across the Al-
1027 tyn Tagh fault zone. *Geophysical Research Letters* 35, L02309,
1028 doi:10.1029/2007GL031511.
- 1029 Jones, L.E., Hough, S.E., 1995. Analysis of broadband records from
1030 the 28 June 1992 Big Bear earthquake: Evidence of a multiple-event
1031 source. *Bulletin of the Seismological Society of America* 85, 688–704.
1032 <http://www.bssaonline.org/cgi/reprint/85/3/688.pdf>.
- 1033 Jónsson, S., 2008. Importance of post-seismic viscous relaxation in southern
1034 Iceland. *Nature Geoscience* 1, 136–139.
- 1035 Jónsson, S., Segall, P., Pedersen, R., Björnsson, G., 2003. Post-earthquake
1036 ground movements correlated to pore-pressure transients. *Nature* 424,
1037 179–183.

- 1038 Jouanne, F., Mugnier, J.L., Gamond, J.F., Le Fort, P., Pandey, M.R.,
1039 Bollinger, L., Flouzat, M., Avouac, J.P., 2004. Current shortening across
1040 the Himalayas of Nepal. *Geophysical Journal International* 157, 1–14.
- 1041 Katsumata, K., Kasahara, M., Ichiyanagi, M., Kikuchi, M., Sen, R.S., Kim,
1042 C.U., Ivaschenko, A., Tatevossian, R., 2004. The 27 May 1995 Ms 7.6
1043 Northern Sakhalin Earthquake: An Earthquake on an Uncertain Plate
1044 Boundary. *Bulletin of the Seismological Society of America* 94, 117–130.
1045 <http://www.bssaonline.org/cgi/reprint/94/1/117.pdf>.
- 1046 Keiding, M., Árnadóttir, T., Sturkell, E., Geirsson, H., Lund, B., 2008. Strain
1047 accumulation along an oblique plate boundary: the Reykjanes Peninsula,
1048 southwest Iceland. *Geophysical Journal International* 172, 861–872.
- 1049 Kirby, E., Harkins, N., Wang, E., et al., 2007. Slip rate gradients along the
1050 eastern Kunlun fault. *Tectonics* 26, TC2010, doi:10.1029/2006TC002033.
- 1051 Kontoes, C., Elias, P., Sykioti, O., Briole, P., Remy, D., Sachpazi, M., Veis,
1052 G., Kotsis, I., 2000. Displacement field and fault model for the September
1053 7, 1999 Athens earthquake inferred from ERS2 satellite radar interferom-
1054 etry. *Geophysical Research Letters* 27, 3989–3992.
- 1055 Koulali, A., Ouazar, D., Tahayt, A., et al., 2011. New GPS constraints
1056 on active deformation along the AfricaIberia plate boundary. *Earth and
1057 Planetary Science Letters* 308, 211–217.
- 1058 Kreemer, C., Holt, W., Haines, A., 2003. An integrated global model of
1059 present-day plate motions and plate boundary deformation. *Geophysical
1060 Journal International* 154, 8–34.

- 1061 LaFemina, P.C., Dixon, T.H., Malservisi, R., Árnadóttir, T., Sturkell,
1062 E., Sigmundsson, F., Einarsson, P., 2005. Geodetic GPS measure-
1063 ments in south Iceland: Strain accumulation and partitioning in a prop-
1064 agating ridge system. *Journal of Geophysical Research* 110, B11405,
1065 doi:10.1029/2005JB003675.
- 1066 Langbein, J., Borchardt, R., Dreger, D., Fletcher, J., Hardebeck, J.L., Hell-
1067 weg, M., Ji, C., Johnston, M., Murray, J.R., Nadeau, R., Rymer, M.J.,
1068 Treiman, J.A., 2005. Preliminary Report on the 28 September 2004, M
1069 6.0 Parkfield, California Earthquake. *Seismological Research Letters* 76,
1070 10–26. <http://srl.geoscienceworld.org/cgi/reprint/76/1/10.pdf>.
- 1071 Larson, K.M., Rurgmann, R., Bilham, R., Freymueller, J.T., 1999. Kinemat-
1072 ics of the India-Eurasia collision zone from GPS measurements. *Journal*
1073 *of Geophysical Research* 104, 1077–1093.
- 1074 Lasserre, C., Peltzer, G., Crampé, F., Klinger, Y., Van der Woerd, J., Tap-
1075 ponnier, P., 2005. Coseismic deformation of the 2001 $M_W = 7.8$ Kokoxili
1076 earthquake in Tibet, measured by synthetic aperture radar interferometry.
1077 *Journal of Geophysical Research* 110.
- 1078 Le Beon, M., Amrat, A.Q., Agnon, A., et al., 2008. Slip rate and locking
1079 depth from GPS profiles across the southern Dead Sea Transform. *Journal*
1080 *of Geophysical Research* 113, B11403, doi:10.1029/2007JB005280.
- 1081 Le Pichon, X., Chamot-Rooke, N., Rangin, C., et al., 2003. The North
1082 Anatolian fault in the Sea of Marmara. *Journal of Geophysical Research*
1083 108, 2179, doi:10.1029/2002JB001862.

- 1084 Li, X., Cormier, V.F., Toksoz, M.N., 2002. Complex Source Pro-
1085 cess of the 17 August 1999 Izmit, Turkey, Earthquake. Bul-
1086 letin of the Seismological Society of America 92, 267–277.
1087 <http://www.bssaonline.org/cgi/reprint/92/1/267.pdf>.
- 1088 Li, Z., Elliott, J.R., Feng, W., Jackson, J.A., Parsons, B., Walters, R.J.,
1089 2011. The 2010 Mw 6.8 Yushu (Qinghai, China) earthquake: Constraints
1090 provided by InSAR and body wave seismology. Journal of Geophysical
1091 Research 116.
- 1092 Li, Z., Feng, W., Xu, Z., Cross, P., Zhang, J., 2008. The 1998 M_w 5.7
1093 Zhangbei-Shangyi (China) earthquake revisited: A buried thrust fault re-
1094 vealed with interferometric synthetic aperture radar. Geochemistry, Geo-
1095 physics, and Geosystems 9.
- 1096 Lohman, R.B., Simons, M., Savage, B., 2002. Location and mechanism of
1097 the Little Skull Mountain earthquake as constrained by satellite radar
1098 interferometry and seismic waveform modeling. Journal of Geophysical
1099 Research 107, 2118.
- 1100 Louvari, E., Kiratzi, A., 2001. Source parameters of the 7 September 1999
1101 Athens (Greece) earthquake based on teleseismic data. Journal of the
1102 Balkan Geophysical Society 4, 51–60.
- 1103 Loveless, J., Meade, B., 2011. Partitioning of localized and diffuse deforma-
1104 tion in the Tibetan Plateau from joint inversions of geologic and geodetic
1105 observations. Earth and Planetary Science Letters 303, 11 – 24.

- 1106 Lyon-Caen, H., Barrier, E., Lasserre, C., et al., 2006. Kinematics of the
1107 North American-Caribbean-Cocos plates in Central America from new GPS
1108 measurements across the Polochic-Motagua fault system. *Geophysical Re-*
1109 *search Letters* 33, L19309, doi:10.1029/2006GL027694.
- 1110 Lyons, S.N., Bock, Y., Sandwell, D.T., 2002. Creep along the Imperial Fault,
1111 southern California, from GPS measurements. *Journal of Geophysical Re-*
1112 *search* 107, 2249, doi:10.1029/2001JB000763.
- 1113 Maggi, A., Jackson, J., Mckenzie, D., Priestley, K., 2000. Earthquake fo-
1114 cal depths, effective elastic thickness, and the strength of the continental
1115 lithosphere. *Geology* 28, 495–498.
- 1116 Maggi, A., Jackson, J.A., McKenzie, D., Priestley, K., 2000. Earthquake
1117 focal depths, effective elastic thickness, and the strength of the continental
1118 lithosphere. *Geology* 28, 495–498.
- 1119 Mahmoud, S., Reilinger, R., McClusky, S., Vernant, P., Tealeb, A., 2005.
1120 GPS evidence for northward motion of the Sinai Block: Implications for
1121 E. Mediterranean tectonics. *Earth and Planetary Science Letters* 238,
1122 217–224.
- 1123 Mahsas, A., Lammali, K., Yelles, K., et al., 2008. Shallow afterslip following
1124 the 2003 May 21, Mw = 6.9 Boumerdes earthquake, Algeria. *Geophysical*
1125 *Journal International* 172, 155–166.
- 1126 Massonnet, D., Feigl, K.L., 1995. Discrimination of geophysical phenomena
1127 in satellite radar interferograms. *Geophysical Research Letters* 22, 1537–
1128 1540.

- 1129 Massonnet, D., Feigl, K.L., Vadon, H., Rossi, M., 1996. Coseismic deformation
1130 field of the M=6.7 Northridge, California earthquake of January 17,
1131 1994 recorded by two radar satellites using interferometry. *Geophysical*
1132 *Research Letters* 23, 969–972.
- 1133 Massonnet, D., Thatcher, W., Vadon, H., 1996. Detection of postseismic
1134 fault-zone collapse following the Landers earthquake. *Nature* 382, 612–
1135 616.
- 1136 Maurin, T., Masson, F., Rangin, C., et al., 2010. First global positioning
1137 system results in northern Myanmar: Constant and localized slip rate
1138 along the Sagaing fault. *Geology* 38, 591–594.
- 1139 Mazzotti, S., Hyndman, R., Flück, P., Smith, A.J., Schmidt, M., 2003. Dis-
1140 tribution of the Pacific/North America motion in the Queen Charlotte
1141 Islands-S. Alaska plate boundary zone. *Geophysical Research Letters* 30,
1142 1762, doi:10.1029/2003GL017586.
- 1143 McKenzie, D., Fairhead, D., 1997. Estimates of the effective elastic thickness
1144 of the continental lithosphere from Bouguer and free air gravity anomalies.
1145 *Journal of Geophysical Research* 102, 27523–27.
- 1146 McKenzie, D., Fairhead, D., 1997. Estimates of the effective elastic thickness
1147 of the continental lithosphere from Bouguer and free air gravity anomalies.
1148 *Journal of Geophysical Research* 102, 27523–27552.
- 1149 McKenzie, D., Jackson, J., Priestley, K., 2005. Thermal structure of oceanic
1150 and continental lithosphere. *Earth and Planetary Science Letters* 233,
1151 337–349.

- 1152 Meade, B., 2007a. Present-day kinematics at the India-Asia collision zone.
1153 *Geology* 35, 81–84.
- 1154 Meade, B.J., 2007b. Present-day kinematics at the India-Asia collision zone.
1155 *Geology* 35, 81–84.
- 1156 Meade, B.J., Hager, B.H., McClusky, S.C., Reilinger, R.E., 2002. Estimates
1157 of seismic potential in the Marmara Sea region from block models of secu-
1158 lar deformation constrained by Global Positioning System measurements.
1159 *Bulletin of the Seismological Society of America* 92, 208–215.
- 1160 Meng, G., Ren, J., Wang, M., et al., 2008. Crustal deformation
1161 in western Sichuan region and implications for 12 May 2008 Ms
1162 8.0 earthquake. *Geochemistry, Geophysics, Geosystems* 9, Q11007,
1163 doi:10.1029/2008GC002144.
- 1164 Metzger, S., Jónsson, S., Geirsson, H., 2011. Locking depth and slip-rate
1165 of the Húsavík Flatey fault, North Iceland, derived from continuous GPS
1166 data 2006-2010. *Geophysical Journal International* 187, 564–576.
- 1167 Moore, M., England, P., Parsons, B., 2002. Relation between surface velocity
1168 field and shear wave splitting in the South Island of New Zealand. *Journal*
1169 *of Geophysical Research* 107, 2198, doi:10.1029/2000JB000093.
- 1170 Motagh, M., Hoffmann, J., Kampes, B., et al., 2007. Strain accumulation
1171 across the Gazikoy-Saros segment of the North Anatolian Fault inferred
1172 from Persistent Scatterer Interferometry and GPS measurements. *Earth*
1173 *and Planetary Science Letters* 255, 432–444.

- 1174 Nakahara, H., Nishimura, T., Sato, H., Ohtake, M., Kinoshita, S., Ham-
1175 aguchi, H., 2002. Broadband Source Process of the 1998 Iwate Prefecture,
1176 Japan, Earthquake as Revealed from Inversion Analyses of Seismic Wave-
1177 forms and Envelopes. *Bulletin of the Seismological Society of America* 92,
1178 1708–1720.
- 1179 Nakamura, T., Tsuboi, S., Kaneda, Y., Yamanaka, Y., 2010. Rupture pro-
1180 cess of the 2008 Wenchuan, China earthquake inferred from teleseismic
1181 waveform inversion and forward modeling of broadband seismic waves.
1182 *Tectonophysics* 491, 72–84.
- 1183 Nazareth, J.J., Hauksson, E., 2004. The seismogenic thickness of the southern
1184 California crust. *Bulletin of the Seismological Society of America* 94, 940–
1185 960.
- 1186 Nishimura, T., Fujiwara, S., Murakami, M., Tobita, M., Nakagawa, H.,
1187 Sagiya, T., Tada, T., 2001. The M6.1 Earthquake triggered by volcanic
1188 inflation of Iwate volcano, northern Japan, observed by satellite radar in-
1189 terferometry. *Geophysical Research Letters* 28, 635–638.
- 1190 Nishimura, T., Imakiire, T., Yarai, H., Ozawa, T., Murakami, M., Kaidzu,
1191 M., 2003. A preliminary fault model of the 2003 July 26, M6.4 northern
1192 Miyagi earthquake, northeastern Japan, estimated from joint inversion of
1193 GPS, leveling, and InSAR data. *Earth, Planets, and Space* 55, 751–757.
- 1194 Nishimura, T., Thatcher, W., 2003. Rheology of the lithosphere inferred from
1195 postseismic uplift following the 1959 Hebgen Lake earthquake. *Journal of*
1196 *Geophysical Research* 108, 2389, doi:10.1029/2002JB002191.

- 1197 Nissen, E., Emmerson, B., Funning, G.J., Mistrukov, A., Parsons, B., Robin-
1198 son, D.P., Rogozhin, E., Wright, T.J., 2007. Combining InSAR and seis-
1199 mology to study the 2003 Siberian Altai earthquakes-dextral strike-slip
1200 and anticlockwise rotations in the northern India-Eurasia collision zone.
1201 *Geophysics Journal International* 169, 216–232.
- 1202 Nissen, E., Yamini-Fard, F., Tatar, M., Gholamzadeh, A., Bergman, E.,
1203 Elliott, J.R., Jackson, J.A., Parsons, B., 2010. The vertical separation
1204 of mainshock rupture and microseismicity at Qeshm island in the Zagros
1205 fold-and-thrust belt, Iran. *Earth and Planetary Science Letters* 296, 181–
1206 194.
- 1207 Nyst, M., Thatcher, W., 2004. New constraints on the active tectonic de-
1208 formation of the Aegean. *Journal of Geophysical Research* 109, B11406,
1209 doi:10.1029/2003JB002830.
- 1210 Oglesby, D.D., Dreger, D.S., Harris, R.A., Ratchkovski, N., Hansen, R., 2004.
1211 Inverse Kinematic and Forward Dynamic Models of the 2002 Denali Fault
1212 Earthquake, Alaska. *Bulletin of the Seismological Society of America* 94.
- 1213 Okada, Y., 1985. Surface deformation due to shear and tensile faults in a
1214 half-space. *Bulletin of the Seismological Society of America* 75, 1135–1154.
- 1215 Ozawa, S., Murakami, M., Fujiwara, S., Tobita, M., 1997. Synthetic aperture
1216 radar interferogram of the 1995 Kobe earthquake and its geodetic inversion.
1217 *Geophysical Research Letters* 24, 2327–2330.
- 1218 Ozawa, T., Nishimura, S., Wada, Y., Ohkura, H., 2005. Coseismic defor-

- 1219 mation of the Mid Niigata prefecture Earthquake in 2004 detected by
1220 RADARSAT/InSAR. *Earth, Planets, and Space* 57, 423–428.
- 1221 Parsons, B., Wright, T., Rowe, P., Andrews, J., Jackson, J., Walker, R.,
1222 Khatib, M., Talebian, M., Bergman, E., Engdahl, E.R., 2006. The 1994
1223 Sefidabeh (eastern Iran) earthquakes revisited: new evidence from satellite
1224 radar interferometry and carbonate dating about the growth of an active
1225 fold above a blind thrust fault. *Geophysics Journal International* 164,
1226 202–217.
- 1227 Pathier, E., Fielding, E.J., Wright, T.J., Walker, R., Parsons, B.E., Hensley,
1228 S., 2006. Displacement field and slip distribution of the 2005 Kashmir
1229 earthquake from SAR imagery. *Geophysical Research Letters* 33.
- 1230 Pearson, C., Denys, P., Hodgkinson, K., 2000. Geodetic constraints on the
1231 kinematics of the alpine fault in the southern south island of New Zealand,
1232 using results from the Hawea-Haast GPS transect. *Geophysical Research*
1233 *Letters* 27, 1319–1322.
- 1234 Pedersen, R., Sigmundsson, F., Feigl, K.L., Árnadóttir, T., 2001. Coseismic
1235 interferograms of two $M_S=6.6$ earthquakes in the South Iceland Seismic
1236 Zone, June 2000. *Geophysical Research Letters* 28, 3341–3344.
- 1237 Peltzer, G., Crampé, F., Hensley, S., et al., 2001. Transient strain accumu-
1238 lation and fault interaction in the Eastern California shear zone. *Geology*
1239 29, 975–978.
- 1240 Peltzer, G., Rosen, P., Rogez, F., et al., 1998. Poroelastic rebound along the

- 1241 Landers 1992 earthquake surface rupture. *J. Geophys. Res.* 103, 30131–
1242 30145.
- 1243 Pérez, O., Bilham, R., Bendick, R., et al., 2001. Velocity field across the
1244 southern Caribbean plate boundary and estimates of Caribbean/South-
1245 American plate motion using GPS geodesy 1994-2000. *Geophysical Re-*
1246 *search Letters* 28, 2987–2990.
- 1247 Pérez-Gussinyé, M., Lowry, A., Watts, A., Velicogna, I., 2004. On the re-
1248 covery of effective elastic thickness using spectral methods: examples from
1249 synthetic data and from the Fennoscandian Shield. *J. Geophys. Res* 109.
- 1250 Perfettini, H., Avouac, J., 2004. Postseismic relaxation driven by brittle
1251 creep: A possible mechanism to reconcile geodetic measurements and the
1252 decay rate of aftershocks, application to the Chi-Chi earthquake, Taiwan.
1253 *Journal of Geophysical Research* 109, B02304, doi:10.1029/2003JB002488.
- 1254 Perfettini, H., Avouac, J., 2007. Modeling afterslip and aftershocks follow-
1255 ing the 1992 Landers earthquake. *Journal of Geophysical Research* 112,
1256 B07409, doi:10.1029/2006JB004399.
- 1257 Peyret, M., Djamour, Y., Hessami, K., et al., 2009. Present-day strain dis-
1258 tribution across the Minab-Zendan-Palami fault system from dense GPS
1259 transects. *Geophysical Journal International* 179, 751–762.
- 1260 Peyret, M., Rolandone, F., Dominguez, S., Djamour, Y., Meyer, B., 2008.
1261 Source model for the Mw 6.1, 31 March 2006, Chalan-Chulan Earthquake
1262 (Iran) from InSAR. *Terra Nova* 20, 126–133.

- 1263 Pezzo, G., Tolomei, C., Atzori, S., et al., 2012. New kinematic constraints of
1264 the western Doruneh fault, northeastern Iran, from interseismic deforma-
1265 tion analysis. *Geophysical Journal International* 190, 622–628.
- 1266 Pollack, H.N., Hurter, S.J., Johnson, J.R., 1993. Heat flow from the earth's
1267 interior - Analysis of the global data set. *Reviews of Geophysics* 31, 267–
1268 280.
- 1269 Pollitz, F., 1992. Postseismic relaxation theory on the spherical earth. *Bul-*
1270 *letin of the Seismological Society of America* 82, 422–453.
- 1271 Pollitz, F., 2003. Transient rheology of the uppermost mantle beneath the
1272 Mojave Desert, California. *Earth and Planetary Science Letters* 215, 89–
1273 104.
- 1274 Pollitz, F., 2005. Transient rheology of the upper mantle beneath cen-
1275 tral Alaska inferred from the crustal velocity field following the 2002
1276 Denali earthquake. *Journal of Geophysical Research* 110, B08407, doi:
1277 10.1029/2005JB003672.
- 1278 Pollitz, F., Bürgmann, R., Segall, P., 1998. Joint estimation of afterslip rate
1279 and postseismic relaxation following the 1989 Loma Prieta earthquake.
1280 *Journal of Geophysical Research* 103, 26975–26992.
- 1281 Pollitz, F., Bürgmann, R., Thatcher, W., 2012. Illumination
1282 of rheological mantle heterogeneity by the M7.2 2010 El Mayor-
1283 Cucapah earthquake. *Geochemistry Geophysics Geosystems* 13, Q06002,
1284 doi:10.1029/2012GC004139.

- 1285 Pollitz, F., Thatcher, W., 2010. On the resolution of shallow mantle viscosity
1286 structure using postearthquake relaxation data: Application to the 1999
1287 Hector Mine, California, earthquake. *Journal of Geophysical Research* 115,
1288 B10412, doi:10.1029/2010JB007405.
- 1289 Pollitz, F.F., Peltzer, G., Bürgmann, R., 2000. Mobility of continental man-
1290 tle: Evidence from postseismic geodetic observations following the 1992
1291 Landers earthquake. *Journal of Geophysical Research* 105, 8035–8054.
- 1292 Prawirodirdjo, L., Bock, Y., McCaffrey, R., et al., 1997. Geodetic observa-
1293 tions of interseismic strain segmentation at the Sumatra subduction zone.
1294 *Geophysical Research Letters* 24, 2601–2604.
- 1295 Priestley, K., McKenzie, D., 2006. The thermal structure of the lithosphere
1296 from shear wave velocities. *Earth and Planetary Science Letters* 244, 285–
1297 301.
- 1298 Pritchard, M.E., Simons, M., Rosen, P.A., Hensley, S., Webb, F.H., 2002.
1299 Co-seismic slip from the 1995 July 30 $M_w = 8.1$ Antofagasta, Chile, earth-
1300 quake as constrained by InSAR and GPS observations. *Geophysics Journal*
1301 *International* 150, 362–376.
- 1302 Reilinger, R., 2006. Evidence for postseismic viscoelastic relaxation follow-
1303 ing the 1959 $M = 7.5$ Hebgen Lake, Montana, earthquake. *Journal of*
1304 *Geophysical Research* 91, 9488–9494.
- 1305 Reilinger, R., McClusky, S., Vernant, P., et al., 2006. GPS constraints on
1306 continental deformation in the Africa-Arabia-Eurasia continental collision

1307 zone and implications for the dynamics of plate interactions. *Journal of*
1308 *Geophysical Research* 111, B05411, doi:10.1029/2005JB004051.

1309 Reilinger, R.E., Ergintav, S., Bürgmann, R., et al., 2000. Coseismic and
1310 postseismic fault slip for the 17 August 1999, M=7.5, Izmit, Turkey earth-
1311 quake. *Science* 289, 1519–1524.

1312 Rigo, A., de Chabaliér, J.B., Meyer, B., Armijo, R., 2004. The 1995 Kozani-
1313 Grevena (northern Greece) earthquake revisited: an improved faulting
1314 model from synthetic aperture radar interferometry. *Geophysics Journal*
1315 *International* 157, 727–736.

1316 Riva, R., Govers, R., 2009. Relating viscosities from postseismic relaxation
1317 to a realistic viscosity structure for the lithosphere. *Geophysical Journal*
1318 *International* 176, 614–624.

1319 Riva, R.E.M., Borghi, A., Aoudia, A., et al., 2007. Viscoelastic relaxation and
1320 long-lasting after-slip following the 1997 Umbria-Marche (Central Italy)
1321 earthquakes. *Geophysical Journal International* 169, 534–546.

1322 Romanowicz, B., Dreger, D., Pasyanos, M., Uhrhammer, R., 1993. Monitor-
1323 ing of strain release in central and northern California using broadband
1324 data. *Geophysical Research Letters* 20, 1643–1646.

1325 Rundle, J., Jackson, D., 1977. A three-dimensional viscoelastic model of a
1326 strike slip fault. *Geophysical Journal of the Royal Astronomical Society*
1327 49, 575–591.

- 1328 Ryder, I., Bürgmann, R., Pollitz, F., 2011. Lower crustal relaxation be-
1329 neath the Tibetan Plateau and Qaidam Basin following the 2001 Kokoxili
1330 earthquake. *Geophysical Journal International* 187, 613–630.
- 1331 Ryder, I., Bürgmann, R., Sun, J., 2010. Tandem afterslip on connected
1332 fault planes following the 2008 Nima-Gaize (Tibet) earthquake. *Journal*
1333 *of Geophysical Research* 115, B03404, doi:10.1029/2009JB006423.
- 1334 Ryder, I., Parsons, B., Wright, T., Funning, G., 2007. Post-seismic motion
1335 following the 1997 Manyi (Tibet) earthquake: InSAR observations and
1336 modelling. *Geophysical Journal International* 169, 1009–1027.
- 1337 Satyabala, S.P., 2006. Coseismic ground deformation due to an intraplate
1338 earthquake using synthetic aperture radar interferometry: The M_w 6.1
1339 Killari, India, earthquake of 29 September 1993. *Journal of Geophysical*
1340 *Research* 111, B02302.
- 1341 Satyabala, S.P., Bilham, R., 2006. Surface deformation and subsurface slip
1342 of the 28 March 1999 $M_w = 6.4$ west Himalayan Chamoli earthquake from
1343 InSAR analysis. *Geophysical Research Letters* 33, L23305.
- 1344 Savage, J., 1990. Equivalent strike-slip earthquake cycles in half-space and
1345 lithosphere-asthenosphere earth models. *Journal of Geophysical Research*
1346 95, 4873–4879.
- 1347 Savage, J., Burford, R., 1973. Geodetic determination of relative plate motion
1348 in central California. *Journal of Geophysical Research* 78, 832–845.

- 1349 Savage, J., Prescott, W., 1978. Asthenosphere readjustment and the earth-
1350 quake cycle. *Journal of Geophysical Research* 83, 3369–3376.
- 1351 Savage, J.C., Svarc, J.L., 1997. Postseismic deformation associated with
1352 the 1992 $M_w=7.3$ Landers earthquake, southern California. *Journal of*
1353 *Geophysical Research* 102, 7565–7578.
- 1354 Scheiber-Enslin, S.E., LaFemina, P.C., Sturkell, E., Hooper, A.J., Webb, S.J.,
1355 2011. Geodetic investigation of plate spreading along a propagating ridge:
1356 the Eastern Volcanic Zone, Iceland. *Geophysical Journal International* 187,
1357 1175–1194.
- 1358 Schmidt, D.A., Bürgmann, R., 2006. InSAR constraints on the source pa-
1359 rameters of the 2001 Bhuj earthquake. *Geophysical Research Letters* 33,
1360 L02315.
- 1361 Scholz, C., Bilham, R., 1991. On the mechanics of earthquake afterslip.
1362 *Journal of Geophysical Research* 96, 8441–8452.
- 1363 Searle, M.P., Elliott, J.R., Phillips, R.J., Chung, S.L., 2011. Crustal-
1364 lithospheric and continental extrusion of tibet. *Journal of the Geological*
1365 *Society of London* 168, 633–672.
- 1366 Seeber, L., Ekström, G., Jain, S.K., Murty, C.V.R., Chandak, N., Arm-
1367 bruster, J.G., 1996. The 1993 Killari earthquake in central India: A new
1368 fault in Mesozoic basalt flows? *Journal of Geophysical Research* 101,
1369 8543–8560.
- 1370 Semmane, F., Campillo, M., Cotton, F., 2005. Fault location and source

1371 process of the Boumerdes, Algeria, earthquake inferred from geodetic and
1372 strong motion data. *Geophysical Research Letters* 32.

1373 Serpelloni, E., Bürgmann, R., Anzidei, M., et al., 2010. Strain accumulation
1374 across the Messina Straits and kinematics of Sicily and Calabria from GPS
1375 data and dislocation modeling. *Earth and Planetary Science Letters* 298,
1376 347–360.

1377 Shelly, D.R., Johnson, K.M., 2011. Tremor reveals stress shadowing, deep
1378 postseismic creep, and depth-dependent slip recurrence on the lower-
1379 crustal San Andreas fault near Parkfield. *Geophysical Research Letters*
1380 38.

1381 Sheu, S.Y., Shieh, C.F., 2004. Viscoelasticafterslip concurrence: a possible
1382 mechanism in the early post-seismic deformation of the Mw 7.6, 1999 Chi-
1383 Chi (Taiwan) earthquake. *Geophysical Journal International* 159, 1112–
1384 1124.

1385 Sibson, R.H., 1982. Fault zone models, heat flow, and the depth distribution
1386 of earthquakes in the continental crust of the United States. *Bulletin of*
1387 *the Seismological Society of America* 72, 151–163.

1388 Simons, M., Fialko, Y., Rivera, L., 2002. Coseismic Deformation from the
1389 1999 Mw 7.1 Hector Mine, California, Earthquake as Inferred from InSAR
1390 and GPS Observations. *Bulletin of the Seismological Society of America* 92,
1391 1390–1402. <http://www.bssaonline.org/cgi/reprint/92/4/1390.pdf>.

1392 Sloan, R.A., Jackson, J.A., McKenzie, D., Priestley, K., 2011. Earthquake
1393 depth distributions in central Asia, and their relations with lithosphere

1394 thickness, shortening and extension. *Geophysics Journal International* 185,
1395 1–29.

1396 Smith, W.H.F., Wessel, P., 1990. Gridding with continuous curvature splines
1397 in tension. *Geophysics* 55, 293.

1398 Smith-Konter, B.R., Sandwell, D.T., Shearer, P., 2011. Locking depths esti-
1399 mated from geodesy and seismology along the San Andreas Fault System:
1400 Implications for seismic moment release. *Journal of Geophysical Research*
1401 116, B06401, doi:10.1029/2010JB008117.

1402 Socquet, A., Simons, W., Vigny, C., et al., 2006a. Microblock rotations and
1403 fault coupling in SE Asia triple junction (Sulawesi, Indonesia) from GPS
1404 and earthquake slip vector data. *Journal of Geophysical Research* 111,
1405 B08409, doi:10.1029/2005JB003963.

1406 Socquet, A., Vigny, C., Chamotrooke, N., et al., 2006b. India and
1407 Sunda plates motion and deformation along their boundary in Myan-
1408 mar determined by GPS. *Journal of Geophysical Research* 111, B05406,
1409 doi:10.1029/2005JB003877.

1410 Soledad Velasco, M., Bennett, R.A., Johnson, R.A., et al., 2010. Subsurface
1411 fault geometries and crustal extension in the eastern Basin and Range
1412 Province, western U.S. *Tectonophysics* 488, 131 – 142.

1413 Spinler, J.C., Bennett, R.A., Anderson, M.L., 2010. Presentday strain accu-
1414 mulation and slip rates associated with southern San Andreas and eastern
1415 California shear zone faults. *Journal of Geophysical Research* 115, B11407,
1416 doi:10.1029/2010JB007424.

- 1417 Stramondo, S., Tesauro, M., Briole, P., Sansosti, E., Salvi, S., Lanari, R.,
1418 Anzidei, M., Baldi, P., Fornaro, G., Avallone, A., Buongiorno, M.F.,
1419 Franceschetti, G., Boschi, E., 1999. The September 26, 1997 Colfiorito,
1420 Italy, earthquakes: modeled coseismic surface displacement from SAR in-
1421 terferometry and GPS. *Geophysical Research Letters* 26, 883–886.
- 1422 Sudhaus, H., Jónsson, S., 2011. Source model for the 1997 Zirkuh earthquake
1423 ($M_W = 7.2$) in Iran derived from JERS and ERS InSAR observations. *Geo-*
1424 *physics Journal International* 185, 676–692.
- 1425 Takeuchi, C., Fialko, Y., 2012. Dynamic models of interseismic deforma-
1426 tion and stress transfer from plate motion to continental transform faults.
1427 *Journal of Geophysical Research* 117, B05403, doi:10.1029/2011JB009056.
- 1428 Talebian, M., Biggs, J., Bolourchi, M., Copley, A., Ghassemi, A., Ghorashi,
1429 M., Hollingsworth, J., Jackson, J., Nissen, E., Oveisi, B., Parsons, B.,
1430 Priestley, K., Saiidi, A., 2006. The Dahuiyeh (Zarand) earthquake of 2005
1431 February 22 in central Iran: reactivation of an intramountain reverse fault.
1432 *Geophysics Journal International* 164, 137–148.
- 1433 al Tarazi, E., Abu Rajab, J., Gomez, F., 2011. GPS mea-
1434 surements of nearfield deformation along the southern Dead Sea
1435 Fault System. *Geochemistry, Geophysics, Geosystems* 12, Q12021,
1436 doi:10.1029/2011GC003736.
- 1437 Tatar, O., Poyraz, F., Gürsoy, H., et al., 2012. Crustal deformation and
1438 kinematics of the Eastern Part of the North Anatolian Fault Zone (Turkey)
1439 from GPS measurements. *Tectonophysics* 518–521, 55–62.

- 1440 Taylor, M., Peltzer, G., 2006. Current slip rates on conjugate strike-slip faults
1441 in central Tibet using synthetic aperture radar interferometry. *Journal of*
1442 *Geophysical Research* 111, B12402, 10.1029/2005JB004014.
- 1443 Tesauro, M., Kaban, M., Cloetingh, S., 2012. Global strength and elastic
1444 thickness of the lithosphere. *Global and Planetary Change* 90–91, 51–57.
- 1445 Thatcher, W., 2007. Microplate model for the present-day deformation of
1446 Tibet. *J. geophys. Res* 112, 1–13.
- 1447 Thatcher, W., England, P., 1998. Ductile shear zones beneath strike-slip
1448 faults: Implications for the thermomechanics of the San Andreas fault
1449 zone. *Journal of Geophysical Research* 103, 891–905.
- 1450 Thatcher, W., Rundle, J., 1979. A model for the earthquake cycle in under-
1451 thrust zones. *Journal of Geophysical Research* 84, 5540–5556.
- 1452 Tobita, M., Fujiwara, S., Ozawa, S., Rosen, P.A., Fielding, E.J., Werner,
1453 C.L., Murakami, M., Nakagawa, H., Nitta, K., Murakami, M., 1998. De-
1454 formation of the 1995 North Sakhalin earthquake detected by JERS-1/SAR
1455 interferometry. *Earth, Planets, and Space* 50, 313–325.
- 1456 Umutlu, N., Koketsu, K., Milkereit, C., 2004. The rupture process during
1457 the 1999 Düzce, Turkey, earthquake from joint inversion of teleseismic and
1458 strong-motion data. *Tectonophysics* 391, 315–324.
- 1459 Utkucu, M., Alptekin, Ö., Pınar, A., 2003. A detailed source study of the
1460 Orta (Çankırı) earthquake of June 6, 2000 (MS = 6.1): An intraplate
1461 earthquake in central Anatolia. *Journal of Seismology* 7, 193–202.

- 1462 Vaghri, A., Hearn, E., 2012. Can lateral viscosity contrasts explain asym-
1463 metric interseismic deformation around strike-slip faults? Bulletin of the
1464 Seismological Society of America 102, 490–503.
- 1465 Velasco, A.A., Ammon, C.J., Beck, S.L., 2000. Broadband source modeling
1466 of the November 8, 1997, Tibet ($M_w = 7.5$) earthquake and its tectonic
1467 implications. Journal of Geophysical Research 105, 28065–28080.
- 1468 Vergnolle, M., Pollitz, F., Calais, E., et al., 2003. Constraints on the viscosity
1469 of the continental crust and mantle from gps measurements and postseismic
1470 deformation models in western mongolia. J. Geophys. Res. 108, 2502.
- 1471 Vigny, C., Socquet, A., Rangin, C., et al., 2003. Present-day crustal defor-
1472 mation around Sagaing fault, Myanmar. Journal of Geophysical Research
1473 108, 2533, doi:10.1029/2002JB001999.
- 1474 Wald, D.J., Heaton, T.H., 1994. Spatial and temporal dis-
1475 tribution of slip for the 1992 Landers, California, earthquake.
1476 Bulletin of the Seismological Society of America 84, 668–691.
1477 <http://www.bssaonline.org/cgi/reprint/84/3/668.pdf>.
- 1478 Walker, R.T., Bergman, E.A., Elliott, J.R., Fielding, E.J., Ghods, A.R.,
1479 Ghoraishi, M., Jackson, J., Nemati, M., Oviesi, B., Talebian, M., Walters,
1480 R., 2013. The 2010–2011 South Rigan (Baluchestan) earthquake sequence
1481 and its implications for distributed deformation and earthquake hazard in
1482 southeast Iran. Geophysics Journal International 193, 349–374.
- 1483 Wallace, K., Yin, G., Bilham, R., 2004. Inescapable slow slip on

- 1484 the Altyn Tagh fault. *Geophysical Research Letters* 31, L09613,
1485 doi:10.1029/2004GL019724.
- 1486 Wallace, L.M., Beavan, J., McCaffrey, R., Berryman, K., Denys, P., 2007.
1487 Balancing the plate motion budget in the South Island, New Zealand using
1488 GPS, geological and seismological data. *Geophysical Journal International*
1489 168, 332–352.
- 1490 Walpersdorf, A., Hatzfeld, D., Nankali, H., et al., 2006. Difference in the
1491 GPS deformation pattern of North and Central Zagros (Iran). *Geophysical*
1492 *Journal International* 167, 1077–1088.
- 1493 Walters, R.J., Elliott, J.R., D’Agostino, N., England, P.C., Hunstad, I., Jack-
1494 son, J.A., Parsons, B., Phillips, R., Roberts, G., 2009. The 2009 L’Aquila
1495 Earthquake (Central Italy): a source mechanism and implications for seis-
1496 mic hazard. *Geophysical Research Letters* 36.
- 1497 Walters, R.J., Holley, R.J., Parsons, B., Wright, T.J., 2011. New signatures
1498 of underground nuclear tests revealed by satellite radar interferometry.
1499 *Geophysical Research Letters* 38, L05303, doi:10.1029/2010GL046443.
- 1500 Wang, H., Wright, T.J., 2012. Satellite geodetic imaging reveals internal
1501 deformation of western Tibet. *Geophysical Research Letters* 39, L07303,
1502 doi:10.1029/2012GL051222.
- 1503 Wang, H., Wright, T.J., Biggs, J., 2009a. Interseismic slip rate of the north-
1504 western Xianshuihe fault from InSAR data. *Geophysical Research Letters*
1505 36, L03302, doi:10.1029/2008GL036560.

- 1506 Wang, L., Wang, R., Roth, F., Enescu, B., Hainzl, S., Ergintav, S., 2009b.
1507 Afterslip and viscoelastic relaxation following the 1999 M 7.4 İzmit earth-
1508 quake from GPS measurements. *Geophysical Journal International* 178,
1509 1220–1237.
- 1510 Watts, A., Zhong, S., Hunter, J., 2013. The behavior of the lithosphere on
1511 seismic to geologic timescales. *Annual Review of Earth and Planetary*
1512 *Sciences* 41.
- 1513 Wdowinski, S., Bock, Y., Baer, G., et al., 2004. GPS measurements of cur-
1514 rent crustal movements along the Dead Sea Fault. *Journal of Geophysical*
1515 *Research* 109, B05403, doi:10.1029/2003JB002640.
- 1516 Wei, S., Fielding, E., Leprince, S., Sladen, A., Avouac, J.P., Helmberger, D.,
1517 Hauksson, E., Chu, R., Simons, M., Hudnut, K., Herring, T., Briggs, R.,
1518 2011. Superficial simplicity of the 2010 El Mayor-Cucapah earthquake of
1519 Baja California in Mexico. *Nature Geoscience* 4, 615–618.
- 1520 Wernicke, B., Davis, J.L., A, B.R., et al., 2004. Tectonic implications of a
1521 dense continuous GPS velocity field at Yucca Mountain, Nevada. *Journal*
1522 *of Geophysical Research* 109, B12404, doi:10.1029/2003JB002832.
- 1523 Wessel, P., Smith, W.H.F., 1998. New, improved version of generic mapping
1524 tools released. *EOS Transactions AGU* 79, 579–579.
- 1525 Weston, J., Ferreira, A., Funning, G., 2012. Systematic comparisons of earth-
1526 quake source models determined using InSAR and seismic data. *Tectono-*
1527 *physics* 532-535, 61–81.

- 1528 Weston, J., Ferreira, A.M.G., Funning, G.J., 2011. Global compilation of in-
1529 terferometric synthetic aperture radar earthquake source models: 1. Com-
1530 parisons with seismic catalogs. *Journal of Geophysical Research* 116.
- 1531 Weston, J., Ferreira, A.M.G., Funning, G.J., 2012. Systematic comparisons
1532 of earthquake source models determined using InSAR and seismic data.
1533 *Tectonophysics* 532–535, 61–81.
- 1534 Wright, T., 2002. Remote monitoring of the earthquake cycle using satellite
1535 radar interferometry. *Philosophical Transactions of the Royal Society of*
1536 *London. Series A: Mathematical, Physical and Engineering Sciences* 360,
1537 2873–2888.
- 1538 Wright, T., Lu, Z., Wicks, C., 2004a. Constraining the slip distribution and
1539 fault geometry of the Mw 7.9, 3 november 2002, Denali fault earthquake
1540 with interferometric synthetic aperture radar and global positioning system
1541 data. *Bulletin of the Seismological Society of America* 94, S175–S189.
- 1542 Wright, T., Parsons, B., Fielding, E., 2001. Measurement of interseismic
1543 strain accumulation across the North Anatolian Fault by satellite radar
1544 interferometry. *Geophysical Research Letters* 28, 2117–2120.
- 1545 Wright, T.J., Lu, Z., Wicks, C., 2003. Source model for the M_w 6.7, 23
1546 October 2002, Nenana Mountain Earthquake (Alaska) from InSAR. *Geo-*
1547 *physical Research Letters* 30.
- 1548 Wright, T.J., Parsons, B., England, P.C., et al., 2004b. InSAR observations
1549 of low slip rates on the major faults of western Tibet. *Science* 305, 236–239.

- 1550 Wright, T.J., Parsons, B.E., Jackson, J.A., Haynes, M., Fielding, E.J., Eng-
1551 land, P.C., Clarke, P.J., 1999. Source parameters of the 1 October 1995
1552 Dinar (Turkey) earthquake from SAR interferometry and seismic body-
1553 wave modelling. *Earth and Planetary Science Letters* 172, 23–37.
- 1554 Yamasaki, T., Houseman, G.A., 2012. The signature of depth-dependent
1555 viscosity structure in post-seismic deformation. *Geophysical Journal In-*
1556 *ternational* 190, 769–784.
- 1557 Yamasaki, T., Wright, T., Houseman, G., 2013. Weak ductile shear zone
1558 beneath a major strike-slip fault: inferences from earthquake cycle model
1559 constrained by geodetic observations of the western North Anatolian Fault
1560 Zone. *Journal of Geophysical Research In Review*.
- 1561 Yang, Z., Chen, W.P., 2008. Mozambique earthquake sequence of 2006: High-
1562 angle normal faulting in southern Africa. *Journal of Geophysical Research*
1563 113.
- 1564 Yelles-Chaouche, A.K., Djellit, H., Beldjoudi, H., Bezzeghoud, M., Buform,
1565 E., 2004. The Ain Temouchent (Algeria) Earthquake of December 22nd,
1566 1999. *Pure and Applied Geophysics* 161, 607–621.
- 1567 Yu, S.B., Hsu, Y.J., Kuo, L.C., et al., 2003. GPS measurement of postseismic
1568 deformation following the 1999 Chi-Chi, Taiwan, earthquake. *Journal of*
1569 *Geophysical Research* 108, 2520, doi:10.1029/2003JB002396.
- 1570 Zhang, P.Z., Molnar, P., Xu, X., 2007. Late Quaternary and present-day
1571 rates of slip along the Altyn Tagh Fault, northern margin of the Tibetan
1572 Plateau. *Tectonics* 26, TC5010,10.1029/2006TC002014.